January 2012

Development Of An Accurate Benchmarking System For Microwave Breast Imaging

Camerin C. Hahn

DEVELOPMENT OF AN ACCURATE BENCHMARKING SYSTEM FOR
MICROWAVE BREAST IMAGING

By

Camerin Hahn
Bachelors of Science, University of North Dakota, 2010

A Thesis
Submitted to the Graduate Faculty

of the

University of North Dakota

In partial fulfillment of the requirements

for the degree of

Masters of Science

Grand Forks, North Dakota
May
2012

This thesis, submitted by Camerin Hahn in partial fulfillment of the requirements for the Degree of Master of Science in Electrical Engineering from the University of North Dakota, has been read by the Faculty Advisory Committee under whom the work has been done, and is hereby approved.

S. Noghanian
Chair person

Edward Santos

Hossein Salehfar

This thesis is being submitted by the appointed advisory committee as having met all of the requirements of the Graduate School at the University of North Dakota and is hereby approved.

Raymond Stidua
Dean of the Graduate School

_5-2-12_
Date

Title   Development of an Accurate Benchmarking System for Microwave Breast
                  Imaging

Department   Electrical Engineering

Degree   Masters of Science

In presenting this thesis in partial fulfillment of the requirements for a graduate degree
from the University of North Dakota, I agree that the library of this University shall make
it freely available for inspection. I further agree that permission for extensive copying for
scholarly purposes may be granted by the professor who supervised my thesis work or, in
her absence, by the Chairperson of the department or the dean of the Graduate School. It
is understood that any copying or publication or other use of this thesis or part thereof for
financial gain shall not be allowed without my written permission. It is also understood
that due recognition shall be given to me and to the University of North Dakota in any
scholarly use which may be made of any material in my thesis.

                                        Camerin Hahn
                                        4/25/2012

TABLE OF CONTENTS

LIST OF FIGURES

LIST OF TABLES

LIST OF SYMBOLS:

Symbol	Description
ε	Permittivity of a material
ε_0	Permittivity of free space
ε_r	Relative permittivity
σ	Conductivity
ω	Radial frequency ($\omega = 2\pi f$)
f	Frequency
j	Representation of an imaginary number ($j = \sqrt{-1}$)
ε_s	permittivity at low frequency
ε_∞	Permittivity at very high frequency
τ_d	Relaxation time
σ_s	Conductivity at low frequency
v	Velocity of a wave traveling in a given medium
λ	Wavelength of a wave traveling in a given medium
c	The speed of light in a vacuum
$\mathbf{E_x}$	Electric field in a given medium polarized in the x direction
$\mathbf{H_y}$	Magnetic field in a given medium polarized in the y direction
η	Intrinsic impedance of a given material
E^+_{x1}	The incident electric field propagating in material 1
E^+_{x2}	An electric field traveling in the same direction as the incident wave but in material 2
E^-_{x1}	The Reflected wave traveling in material 1
Γ	Reflection coefficient
τ	Transmission coefficient
DF	Degrees of Freedom
VNA	Vector Network Analyzer
MS	Mean Squared
SS	Sum of Squares
P	Power of the regression equation
F	Power normalized to an F distribution
a	Regression equation calculated constants
b	Regression equation calculated constants
c	Regression equation calculated constants
d	Regression equation calculated constants
m	Mass of the material in question

Symbol	Description
STD	Standard Deviation
ε_{Debye}	Permittivity calculated from Debye model
$\varepsilon_{Regression}$	Permittivity calculated from Regression model
σ_{Debye}	Conductivity calculated from Debye model
$\sigma_{Regression}$	Conductivity calculated from Regression model
L	Inductance
C	Capacitance
R	Resistance
ASIC	Application Specific Integrated Circuit
$\varepsilon_{Material}$	Permittivity of oscillation while measuring material
ε_{Water}	Permittivity of oscillation while measuring water
ε_{Norm}	Normalized permittivity
$f_{Material}$	Frequency of oscillation while measuring material
f_{Water}	Frequency of oscillation while measuring water
f_{Norm}	Normalized frequency
$\varepsilon_{Measured}$	Estimated dielectric properties
$f_{Measured}$	Frequency of oscillation while measuring
$\varepsilon_{Capacitive\ Method}$	Permittivity measured by capacitive sensor
$\varepsilon_{Capacitive\ Method}$	Permittivity measured by commercial probe

ACKNOWLEDGEMENTS

To: Jerry and Lori Hahn

ABSTRACT

This thesis is a discussion of the design and implementation of benchmarking system for microwave imaging systems. The current benchmarking tools for microwave imaging setups are not adaptable. A novel method for of the development of a dielectric phantom using regression analysis is presented. This is followed by a discussion of the design of a novel sensor for the purpose of *in vivo* dielectric properties measurements. The goal is to provide information for microwave tomography algorithms and phantom development based on *in vivo* dielectric properties of breast tissues

Through the progress of this research two major novel advances have been made toward producing a better microwave imaging benchmark. First, a technique for systematically developing a breast phantom using regression analysis has been developed. This defines a process for researchers to produce a phantom quickly and easily, avoiding the simple trial and error development techniques of the past. Secondly, a method for measuring dielectric constant of a material through an embedded sensor was developed. Both advances are very important in producing accurate phantoms, providing *in vivo* tissue properties for tomography algorithms and designing matching materials for microwave imaging.

CHAPTER 1: INTRODUCTION

In the field of breast cancer detection and imaging, a researcher community is developing microwave imaging setups with the goal of reducing the false-positive as well as the false-negative rates that are associated with the mammography [1]-[4]. These ideas are fundamentally developed upon the assumption that a contrast between malignant and benign tumors exists [2], [3]. This assumption is based upon wide spread tissue measurement of excised tissue [5]-[7]. This contingent is made up of different groups. Usually each group develops its own imaging setups, algorithms, and benchmarking materials. This thesis concentrates upon this subject and aims to create a phantom that can be easily adapted to fit the benchmarking needs for this research contingent as data emerges.

1.1 Motivation

The independent development of all different microwave imaging systems renders comparisons between the very difficult. Different research groups have developed benchmarking systems. Furthermore, many times the algorithms and hardware have tested repeated on models that differ from human breast tissue. Due to the lack of a standardized, dielectrically accurate phantom evaluation and assessment of different imaging system is very difficult, if possible at an. To remedy this problem, some researchers have started to develop specific and specialized test materials to build realistic models of breast tissue [8]-[10]; these models will be referred to as phantoms for

the remainder of this thesis. These phantoms are based upon the measurements of excised tissue and are typically designed to function as a breast analog for a specific frequency range. Some examples of phantoms are published in [8]-[10]. The methods for developing these phantoms typically are not discussed. In some papers a phantom for a standard benchmark for the various imaging setups has been recommended [11]. Due to the unknown development process, these phantoms are static and cannot be updated if advancements are made in the measurement of the tissue being mimicked. To confound this problem, recent work has been shown that measurements of tissue can change substantially within the first few minutes of excision [12]-[14]. As new and more accurate phantoms are being developed procedures to develop a standard benchmark system also has to be addressed

This thesis is a step towards developing a systematic approach in phantom development, as well as producing a method for collecting data of *in vivo* tissue. As mentioned before, the benchmark should be easily adapted. For this purpose, a regression based approach has been chosen for phantom development. This process allows the researcher to follow a controlled method to phantom development, and eliminate wasted experiment time in the development of new phantoms every time a new set of measurements are taken. With this method of building phantoms, it is possible to adapt the phantom as more data regarding the *in vivo* dielectric properties emerges.

With studies being completed on the dielectric properties on excised tissue, some have hypothesized that the dielectric properties change due to several changes that occur during surgery: loss of blood flow, change in temperature, evaporation, etc. To mitigate these changes, *in vivo* measurements are required. Ideally, to measure these dielectric

2

properties, the measurement devices must be wireless, biocompatible, low power, and small. In this thesis a technique to measure the dielectric properties with an embedded sensor is discussed. The goal was to design a low power, biocompatible, small size that can be easily adapted to wireless transmission.

To test this measurement techniques accuracy, several different dielectric materials were measured. After initial testing and verification, this sensor was placed inside several unknown dielectrics and the permittivity was measured and calculated. This measurement was then compared to measurements taken with a commercial dielectric properties probe. The future direction of this work includes an animal study using a wireless embedded sensor.

1.2 Thesis Outline

Literature Review

In this section the important properties and ideas that motivated and driven this thesis are discussed. This provides an introduction to the subject of dielectric properties measurement and biological sensors, and discusses the ideas associated with replicating human tissues for testing different electromagnetic systems.

Dielectric Phantom Development

In the second chapter of this thesis a new technique for producing a phantom that matches the dielectric properties of human breast tissue is described. A simple regression model to estimate the dielectric properties of a given mixture is used as guidance to create materials that can match the test requirements. In this thesis, the breast phantom is

made of a mixture of gelatin, water, propylene glycol and oil. However, this technique can be extended to other mixtures by changing material choices.

Sensor Development

Even though phantoms are developed to closely model human breast tissue, the designs are referenced to respect to *ex vivo* tissue properties. There is a need for a large-scale *in vivo* tissue property measurement. *Ex vivo* properties measurements are usually carried out a few minutes after the tissue is excised. This process causes error to be introduced while the tissue is being removed from the body, or during the time between excision and measurement. To collect *in vivo* tissue properties, measurements should be completed with the sensor embedded inside of the live tissue. Therefore in Chapter 4 we propose a biocompatible wireless sensor. The development of such a sensor can also provide a database of tissue properties needed for imaging algorithms used in microwave tomography.

Future Work and Conclusions

The future directions of the project are discussed in Chapter 5. There are several steps left before getting to a complete benchmarking system that were beyond this thesis and are left for future studies.

CHAPTER 2: LITERATURE REVIEW

Materials can be categorized into two groups based upon their dielectric properties: conductors and dielectrics. The focus here is the design and characteristics measurement of dielectric materials. Contrary to conductors, dielectrics have limited or no free electrons that allow for the flow of current. As an electric field is applied to dielectrics, electric dipoles are formed in the medium and are aligned with this electric field. The resistance to this change is typically referred to as the permittivity of the material [15]. This section is a discussion of the physical meaning, mathematical representation, dispersive nature, measurement techniques, and possible causes of variations in the permittivity of a dielectric material.

2.1 Theoretical Representation

The dielectric properties of a material can be reduced down to three fundamental characteristics: conductivity (σ), permittivity (ε), and permeability (μ). Here our focus is on permittivity and conductivity. The permeability of a material is only relevant for magnetic materials. All materials discussed in this thesis are assumed to be non-magnetic. This means that their permeability is the same as free space ($\mu=\mu_0$). To begin the discussion of dielectrics, we will also assume that the conductivity of the dielectric is negligible (lossless materials. The permittivity of a lossless dielectric can be represented as in Equation (1).

$$\varepsilon = \varepsilon_r \varepsilon_0$$

ε = Permittivity

ε_0 = Permittivity of free space

(1)

ε_r = Relative permittivity or dielectric constant

The dielectric constant is dependent upon the material properties. Up to this point we have assumed that the dielectric material in question is lossless. For a lossy dielectric, conductivity is not negligible. To include this, a complex conductivity is defined as part of the permittivity; this is shown in Equation (2). σ is the conductivity and ω is the angular velocity of a wave traveling through the material [15].

$$\varepsilon = \varepsilon_0 \left(\varepsilon' - j\varepsilon'' \right) = \varepsilon_0 \left(\varepsilon_r - \frac{j\sigma}{\omega \varepsilon_0} \right)$$

σ = Conductivity

(2)

ω = Radial frequency = $2\pi f$

f = Frequency

2.1.1 Dispersive Nature of Dielectrics

It is important to notice that each dielectric constant has a "relaxation time". This means that polarization of the dielectric takes some time to become completely aligned. Depending upon the frequency of the external electric field, the dielectric may not become fully polarized. This partial polarization causes changes in the dielectric properties of the material. The frequency dependence of permittivity is referred to as "dispersion". The dielectric properties of interest in microwave imaging are within the frequency range of 0-20GHz. Human tissue exhibits dispersion within this band. This dispersion can be characterized by the Debye model. The first order Debye model is given in Equation (3). In this model ε_∞ is the permittivity at infinity (in practice, this is the permittivity of the highest frequency we can measure), ε_s is the permittivity at a very low frequency. The symbol τ represents the relaxation time.

6

$$\varepsilon(\omega) = \varepsilon_\infty + \frac{\varepsilon_s - \varepsilon_\infty}{1 + j\omega\tau_d} - j\frac{\sigma_s}{\omega\varepsilon_0}$$

ε_s = Permittivity at low frequency (3)

ε_∞ = Permittivity at very high frequency

σ_s = Conductivity at low frequency

τ_d = Relaxation time

2.2 Electromagnetic Wave Interaction with Dielectrics

As a wave travels through a dielectric, the speed of the wave is reduced. The wave velocity is proportional to dielectric constant as shown in Equation (4) [15]. In Equation (4), c is defined as the speed of light in a vacuum, and μ is the magnetic permeability. As mentioned before human tissue is nonmagnetic, therefore, permeability is the same as free space permeability. Along with the speed of the wave, the ratio of the magnitude of the magnetic field and electric fields are dependent upon the dielectric properties. This ratio of magnitudes is known as the intrinsic impedance of the material (η). The intrinsic impedance is defined in Equation (5). When a wave in a dielectric travels toward an interface between two dielectric materials, it is referred to as the incident wave. The discontinuity causes a portion of the wave to be and a portion to be reflected. In Equation (6) E_{x1}^+ is the magnitude of the incident electric field. In Equation (7) E_{x2}^+ is the magnitude of the transmitted electric field. The incident wave is related to the transmitted and reflected waves through the reflection co-efficient Γ and the transmission co-efficient τ, respectively.

$$v = \frac{1}{\sqrt{\mu\varepsilon}} = \frac{1}{\sqrt{\mu_0\varepsilon_0\varepsilon_r}} = \frac{c}{\sqrt{\varepsilon_r}}$$

(4)

v = Velocity of a wave traveling in a given medium

c = The speed of light in vacuum

7

$$\frac{E_x}{H_y} = \eta = \sqrt{\frac{\mu}{\varepsilon}}$$

E_x = Magnitude of electric field in a given medium polarized in the x direction   (5)

H_y = Magnitude of magnetic field in a given medium polarized in the y direction

η = Intrinsic impedance of a given material

$$\Gamma = \frac{E_{x1}^-}{E_{x1}^+} = \frac{\eta_2 - \eta_1}{\eta_2 + \eta_1}$$

E_{x1}^- =The magnitude of incident electric field propagating in material 1   (6)

E_{x1}^+ = The magnituded of reflected electric field traveling in material 1

Γ = Reflection coefficient

$$\tau = \frac{E_{x2}^+}{X_{x1}^+} = \frac{2\eta_2}{\eta_1 + \eta_2} = 1 + \Gamma$$

(7)

E_{x2}^+ = Magnitude of the transmitted field traveling in material 2

τ = Transmission coefficient

2.3 Dielectric Properties Measurement

In microwave imaging, knowledge of tissue dielectric properties is essential. Therefore, a review of measurement techniques is given here. The most important measurement techniques can be categorized into two broad categories: cavity, and transmission line. In the cavity technique, the dielectric properties are calculated by measuring the changes in the cavity properties due to dielectric loading and comparing them to theoretical models. The transmission line technique uses the wave reflections and transmissions in a particular dielectric filled line to determine the properties of the material. The interactions with the dielectric can be measured across a spectrum. A breakdown of the classifications and relationships between different measurement techniques is shown in Figure 1.
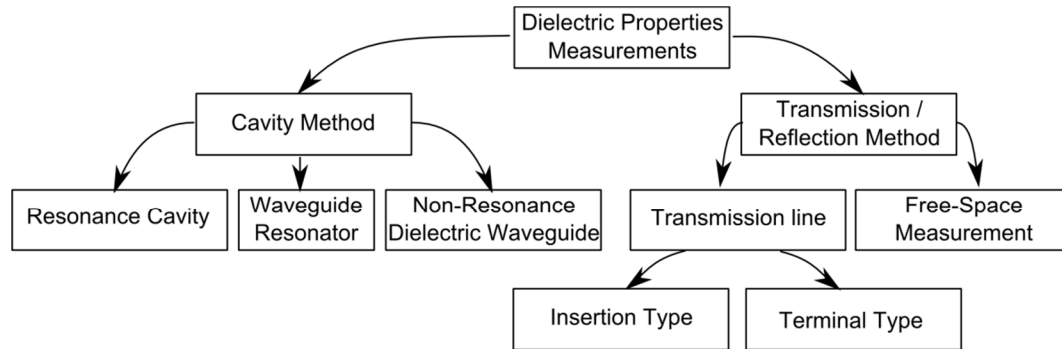
Figure 1: A depiction of the measurement categorization and organization.

2.3.1 Overview of Cavity Measurement Techniques

The cavity measurement techniques generally relate a measured resonant frequency to a set of equations derived for a theatrical model of an identical setup. Due to the close ties to electromagnetic theory, these techniques have been considered extremely precise. This method has been used to establish accepted values of the permittivity of several materials. In some cases it has even been used for tissue studies [16].

Resonance Cavity

Resonance cavity is considered very precise for measuring the dielectric properties. This method shows a very close and accurate relationship to theoretical models. However, this method is not without its limitations. A cavity must be designed for each frequency that data of interest [17]. The construction and design of a set of cavities for measuring dielectric properties can be long and arduous even for a small bandwidth. The second major shortcoming of this method is the theoretical requirement of a truly homogeneous sample. This requirement limits the measurement candidate to materials small enough to be considered homogeneous [17]. If the sample is not uniform it is not possible to calculate the permittivity with this method. The third shortcoming of this measurement method is that only the magnitude of the permittivity of the material

can be calculated; the information gathered is not sufficient to calculate the complex permittivity. Due to these limitations, the use of this method has typically been limited to characterization of standard liquid solutions, such as distilled water or alcohol [18]. These materials have since been used to calibrate and assess the accuracy of other methods of measuring dielectric properties. This method has been used to characterize the dielectric properties in some limited studies [16], [19].

Waveguide Resonator

To reduce the number of cavities that must be built the waveguide resonator was created. This technique uses a waveguide that has a short circuit termination at one end and another short circuit that may be moved at the opposing end of a waveguide. A uniform dielectric can be inserted transversely into the waveguide. This will create a cavity with a variable volume. When the dielectric is inserted the resonance frequency of the cavity will change, and this change in resonance frequency is used to measure the dielectric properties. The dielectric is placed on a micrometer and moved down the waveguide until initial resonance is established. Then the dielectric is moved down the waveguide until resonance is reestablished [17]. These measurements are compared to theoretical models and thereby the dielectric properties are calculated.

Non-Resonance Dielectric Waveguide

This method is modeled as a resonator between two parallel plates. Non-resonance dielectric waveguide does not require the resonance of the material, but the material must be shaped appropriately. This method uses the vertical propagation of a wave through the material and free space to determine dielectric properties of the material. In this method multiple measurements may be taken with one sample and one

cavity. This provides the additional benefit of requiring fewer cavities to provide a broad band measurement [17].

2.3.2 Reflection/Transmission Technique

The reflection transmission techniques can be divided into two major categories of transmission line and free-space measurements. The transmission line technique is more accurate than the free-space technique, but requires much more equipment and care when taking measurements. The transmission line measurements are taken by placing the dielectric in question in the path of the transmission line and measuring either the transmission or reflection coefficients. The free-space measurement technique is the least precise method; however, it is the least destructive method. All of the transmission and reflection techniques provide the broadband characterization of the material with varying degrees of accuracy [17].

Transmission Line

For this measurement process a modified transmission line is required, which can be a waveguide, coaxial line, micro-strip line, or other types of transmission line. The transmission lines are connected to a network analyzer and measurements are taken while loaded with the dielectric and with some calibration materials. Typical calibration include: air, short circuit, and distilled water. The reflection coefficient is measured across a frequency spectrum. Calculations are completed in post processing by comparing the reflection coefficient of the unknown material to that of the known calibration materials [17]. On major advantage of this method is the benefit of being able to measure the complex permittivity. However, this technique requires the use of a Vector Network

Analyzer (VNA) for complex permittivity. A scalar network analyzer can be used if only relative permittivity is needed [17].

Overview of Methods

The transmission line technique can have two different methods of loading. The first method simply creates a smooth break in the line for the material to contact, referred to as "terminal type". The second method creates a void in the transmission line, where the dielectric is placed as part of the transmission line for some distance, referred to as "insertion type". Both types have good precision, but the degrees of material destruction may vary [17].

Insertion Type

Two cases will be considered, one case for which the unknown dielectric fills the entire cavity, and the other where the dielectric partially fills the gap in the transmission line. If the material fills the entire area, an analytical solution can be derived depending on the size and shape of the loaded area. This allows for simple, quick and precise calculation of the material's dielectric properties. If the material does not fill the entire area, then an analytical solution may not be reached and an iterative solver may be used to estimate the dielectric material, reducing the precision of this method greatly. One major problem with this method is the fact that when solving for the dielectric properties multiple solutions may exist. This problem only exists in sample larger than $\lambda/2$, where λ is the wavelength of the traveling wave in the material. This limits the range for which the dielectric properties can be precisely measured. However, this method is commonly used with waveguide measurements due to the ease of fabrication and the inherent hollow area in the waveguide. Due to the fact that material must fill a gap completely, the

material is typically the sample material is only useful during the measurements discarded afterwards [17].

There have been many different structures used for this type of measurement including: two waveguides of different lengths and completely filled with the unknown dielectric materials, and a filled cylinder, and surrounded severed lines. The parallel waveguide technique allows for the direct calculations of the dielectric properties without providing multiple solutions. This method has little calibration due to the fact that measurements are differential and are depended on the waveguides. The downside of this method is clearly the amount of material required as well as the destructive nature of the process. The filled cylinder technique is derived from a number of measurements taken from known dielectrics and forward solving to product a model using the transmission and reflections scattering parameters. This method is very simple to calculate and avoids the inherent inverse problem that is involved with some of other techniques. The major problems with this method include: large amounts of calibration to find the solution, as well as destructive nature of the insertion type measurement. The shrouded severed line is a terminal line measurement that uses an extended ground shroud to allow for analytical solutions. This method only requires the reflection coefficient, an angle of reflection for the material, and some calibration material. As with all of the insertion type probes, this is a destructive method, but provides more precise results [17].

Terminal Type

The terminal type measurement is the most commonly used measurement technique. This method is less destructive, while having the ability of broadband complex permittivity measurements. The probe for measuring dielectrics in this manor is typically

a severed coaxial line. At the end of this line a smooth, typically polished surface will make contact with a large sample of the dielectric material. At the interface, the wave traveling along the transmission line will be partially reflected and partially transmitted. By the measurement of the reflected wave the complex permittivity can be calculated. This technique requires some calibration measurements and a smooth, gap-free contact to the dielectric. If there is a gap between the materials the measurements will be inaccurate. This method also requires a large size sample. If the sample is not sufficiently large, multiple reflections may occur, and these multiple reflections will reduce the accuracy. The required size is dependent upon the design of the probe and the dielectric properties of the material. This method is commonly used due to the simple setup, measurement accuracy, the ability to calculate the complex permittivity, and the non-destructive nature of the measurement [17].

Free-Space Measurements

Free space measuring is the least precise method for measuring the dielectric properties. The measurement setup typically consists of one transmission antenna and one reception antenna directed toward each other with a sheet of dielectric in between. To reduce the effects of multipath signals, absorbers are typically placed along the transmission path to attenuate these reflections. The calculations are completed via the transmission and reflection coefficient generated by the sheet of material. This method typically assumes an infinite sheet of dielectric material. The inherent inaccuracy of this method is due to these assumptions. The assumption of no multipath signals is not always accurate, as well as the assumption of an infinite sheet in the calculations. These assumptions add a small error, however in applications that do not require precision these

errors are not significant. The primary advantage of this technique is the simple setup and the non-destructive nature of it. This technique has been used for measuring the permittivity of grain, soil, or other materials that require quick measurements and a large amount of material is available [17].

2.4 Dielectric Properties of Biological Tissues

As dielectric properties measurements have advanced, researches have made an effort to characterize many materials, including many biological tissues. One of the largest studies regarding the characterization of human tissue is divided into three papers [5]-[7]. In these studies, tissues were excised and measured over 10 Hz to 20 GHz spectrum. This study has been widely used for testing and prototyping devices to function around or inside of humans. This study used exclusively *ex vivo* tissue, but characterized most of the human tissues types. In recent years, some limited studies were done on *in vivo, in vitro* and *ex vivo* human and animal tissues [8], [20]-[22].

2.4.1 Measurement Techniques for Dielectric Properties of Tissue

Measuring the dielectric properties of biological tissues is not a trivial project. Researchers need a large database of accurate data; the pursuit of new information must to be balanced with preserving the tissue for further study. Some groups have used the resonant cavity technique [16], but this method requires the tissue to fit a certain shape, and effectively destroys the tissue for future research and only measures the dielectric properties at one frequency [16]. Many groups choose the less invasive coaxial probe technique, allowing for accurate and broadband measurements [5]-[7], [21], [23]-[24].

When the measurements are transitioned from *ex vivo* to *in vivo*, the probes need to be designed for biocompatibility [24].

Biocompatibility

Biocompatibility is an issue when measuring tissues within the living organism. When designing any device that will interact with the body, including a dielectric properties probe, the body's response to the device must be assessed. In the body there are two immune response systems: innate immune system and adaptive immune system. These two immune reactions are very different in their functionality [25]. In the case of dielectric properties probes we are interested in the innate response, not the adaptive response as the adaptive response primarily relates to pathogens. The innate immune system is the initial reaction. This process will happen with any wound regardless of it becoming infected or not [26]. This innate response is divided into sub responses: acute response and chronic response [25]. The acute response consists of a swelling and the localized preventative increased immune response. It can be assumed that the swelling and the increased immune response can affect the measurement of the tissue in question. The chronic response is the long term response of the tissue to the wound. In the case of measuring dielectric properties, this response should be minimized for the comfort of the subject as well as the integrity of the measurements.

Biocompatible Materials

To allow for measurements inside of the body, materials chosen to construct the probe must be biocompatible, meaning that the body either responds favorably or does not respond at all to the material used. Biocompatible materials can be divided into three subcategories: resorbable, encourage growth, inert [25]. In the case of dielectric probes,

resorbable materials and materials that encourage growth will either change the measurement by attaching to the probe or dissolving portions of the probe during the measurement process. These materials are typically avoided due to inconsistencies in the measurements. Dielectric probes often are produced from inert metals and dielectrics such as glass or stainless steel [24]. These materials do not encourage growth or discourage it, and do not cause an increased immune response.

Physiological Changes after Excision

As with any injury, the body reacts to surgery in a variety of ways. Some of these reactions may affect the dielectric properties of the tissues. This section will discuss some of the typical responses that a body may have during the surgery. Some of the effects of surgery include: activation of the sympathetic nervous system, endocrine stress response, and an immune response [27]. The sympathetic nervous system causes an irregular and heightened heart rate [14]. During the endocrine stress response, an increase in release of stored food and other pro-growth materials into the subject's system promotes healing [14]. The immune system of the subject will react to the surgery as well, and the surgery can cause an increase in macrophages as well as acute swelling to the tissue in the area [26]. Each of these mechanisms could affect the dielectric properties of the tissues under measurement.

Implantable Sensors

Generally, sensors have been developed for measuring different properties of various biomedical signals. These sensors range in function from measuring pH or pressure to measuring neural impulses. Some of these sensors have implemented a wireless link [28]-[33], while other sensors are still implanted temporarily and attached to

17

larger equipment [34], [35]. Currently, the only sensor, that we are aware of, which can measure dielectrics without wires only allows for measurement to a depth of a few micro meters [36]. As for the measurement of dielectric properties, we have found no sensor that can adequately assess the dielectric properties of a tissue while implanted inside the body.

2.4.2 Tissue Mimicking Materials: Phantoms

When testing new equipment that has not yet been approved for use with biological subjects, it is common practice to use a synthetic material substitute for the biological subject [23], [37]-[52]. These tissue mimicking materials are often referred to as phantoms. In many cases these phantoms mimic the body with respect to size [37], shape [37], density [38], or in the case of electromagnetic devices, dielectric properties [8]-[10], [39]-[41], [51]. These phantoms are mainly used for the benchmarking new imaging and biomedical devices.

Uses for Dielectric Phantoms

As stated, dielectric phantoms are synthetic materials that are designed to electrically represent tissue. Many fields require dielectric phantoms to substitute biological test subjects including: microwave imaging [8]-[10], [39]-[42], RF ablation testing [43]-[46], antenna testing [47]-[49], implanted product testing [50]-[51], and many others. Each of these devices requires differing levels of accuracy for the phantom to be useful.

Microwave Imaging

Measurements of biological tissues have shown that the dielectric properties vary substantially by tissue type [5]-[7]. This contrast will cause a reflection at the point of contrast as depicted in Equation (6). Microwave imaging is the process of mapping the inferred dielectric properties of an area from the scattered field measurements. The concept of using microwave imaging for cancer detection is based upon identifying areas with large contrast between the dielectric properties of malignant tumors, benign tumors, and healthy tissue causing these reflections [21], [23]. Many research groups have attempted to construct a system for the detection tumors through the contrasts in the dielectric properties of breast tissues. The methods used by these groups can be divided into two categories: radar imaging and tomography [52].

Radar Imaging

The radar method maps the scattering coefficients for the material in question into 2 or 3 dimensional images [39], [40]. In theory, the large scattering coefficient indicates a high contrast in dielectric properties. Due to the nature of radar imaging, only the contrast between two adjacent media is determined, and the magnitude of the permittivity of the material is not calculated. Thereby some active research groups in radar imaging use phantoms that consist of common materials with contrasts similar to that of the contrast of breast tissue. This method finds only high contrast areas and calculates the reflections at these contrast areas. For the purpose of breast cancer detection, it is important to quantify the permittivity to properly categorize tumors as malignant or benign [5]-[7]. The problems with radar imaging have made the tomography technique a popular research topic for current microwave imaging research.

Tomography

When producing a tomographic image, a source is placed on one side of the object, and receivers are placed on the opposite side of or around the object. The scattered field is measured, and from this data the unknown object's profile is found. The object is then rotated and a second image is formed. This process is iterated to produce a set of images from each side of the object. A 3 dimensional image can be constructed by compiling sets of two dimensional images [41], [52]. This process is more computationally intensive than the traditional radar method, but a map of the dielectric properties is produced rather than a map of the contrasts. From the map of dielectric properties, and by comparison with dielectric properties of *in vivo* tissues, the image of tissues regions are constructed. This method requires a much more realistic phantom to prove its functionality [9]-[10]. This phantom should closely match the permittivity and conductivity of the material in question as well as the structure of the material.

Imaging Algorithms

The microwave tomography is an inverse problem that is based on a system of under defined equations. This means that more unknown variables exist than equations necessary to solve for the variable. With an ill-posed problem such as this, the process to solve the equation requires optimization and approximations. The optimization of the ill-posed system is a very computationally intense process. Different optimization techniques provide varying degrees of precision and each assumption provides a degree of inaccuracy [8], [39]-[42], [52]. To simplify the tomography calculations, different approximations have been made. One common approximation for the tomography is the Borne approximation [3]. This approximation assumes the changes in dielectric

properties are relatively small. The second approximation operates by assuming that the dielectric properties in the object of interest are within a given range. For this method it is important to have a well-defined range for these dielectric properties. The need for this well-defined range has prompted a set of studies to accurately assess the *in-vivo* dielectric properties of breast tissue. To assess the improvement in these algorithms, many groups have developed phantoms that work for their purposes, but due to the range of imaging setup these phantoms cannot be used to compare the work of multiple groups [3]. Due to the lack of a broadband anatomically correct phantom the comparisons between different groups is nearly impossible.

Imaging Setups

Different research groups have developed different imaging setups. Some groups have chosen to use large test chambers to facilitate a far-field assumption, while others have chosen to reduce the size to allow for better signal strength. Some groups have chosen narrow band antennas such as simple monopole, or dipole antenna to simplify the imaging algorithms [39], while others have chosen to use wideband directive antennas, such as Vivaldi and double ridge horn antennas [9]. Each of these choices comes with benefits and costs to be assessed. Increasing the number of antennas will increase the amount of data available for producing the image and reducing the possibility of ill-posed problems. But more data means more computations along with a more problems such as mutual coupling or phase errors. Due to limitations on power and high conductivity of skin, antennas should be as close as possible to the object; also matching liquids should be used. Each of these imaging setups costs thousands of dollars and the assessment of

each of these setups should be completed upon a standard material for a better understanding of the problems associated with each measurement setup.

Current Dielectric Phantoms

Many different groups have designed phantom for various frequencies and various bandwidths. Some of these dielectric phantoms are designed to accurately match the dielectric properties of the tissue in question [8]-[10], [42] while others simply match the contrast between the tissues in question. Depending upon the application, the structure of these phantoms varies from solid blocks [40]-[41], to gelatins [8]-[10], [42], and to liquid phantoms [39]. These phantoms vary from matching only permittivity over a narrow frequency band, to matching complex permittivity for ultra wideband applications [10].

2.5 Conclusion

This thesis is a discussion of building an accurate dielectric phantom. This literature review has been written to introduce the reader to concepts of dielectric properties measurements and the basics of microwave imaging. This information will help the reader understand the following discussion regarding the development of a dielectric phantom, as well as the development of dielectric properties sensor. The following chapter discusses the design process for producing a dielectric phantom for microwave imaging.

CHAPTER 3: DIELECTRIC PHANTOM DESIGN

As discussed previously, a dielectric phantom is an analog for biological tissue that would otherwise be endangered by or complicate the test of an emerging system. This chapter discusses a systematic approach to developing a phantom for the purpose of testing microwave imaging setups. This approach uses the linear regression to model to the dielectric properties with variations respect to a change in chemical contents.

3.1 Introduction

A major problem in developing a microwave imaging systems for tumor detection is the lack of standards in benchmarking these systems using a dielectrically accurate human analog. Many researchers use objects that are physically or dielectrically dissimilar to human tissue [39]-[41]. There are a few phantoms based on heterogeneous and dispersive breast tissue dielectric properties presented in literature [8]-[10], [42]. It is important to be able to match the dielectric properties for a variety of tissues over a span of frequency band. Therefore, a systematic method for creating a mixture with desired dielectric properties was needed. This method should provide a procedure to find the required amount of each material in the mixture to match the desired permittivity and conductivity for a given frequency band. We present an approach based on regression model to create mixtures that are both dielectrically similar, and represents accurate physical and physiological properties of breast tissues.

23

Multivariable regression analysis was used to approximate the dielectric properties based upon the contents of a chemical mixture, due to a nonlinear relationship between chemical content of mixtures and their dielectric properties. The regression model for this process was generated by analyzing several mixtures and the changes in their dielectric properties. To produce these data sets, four materials types with varying masses were considered and their conductivity and permittivity were measured. Multivariable regression analysis was performed on this set of mixtures, and the results were used to predict a mixture with desirable dielectric properties. The measured results and chemical contents were added to the database and used to generate the regression equations. This process was repeated until a suitable mixture with broadband dielectric match was developed.

3.2 Material Selection and Methodology

The research in [10] revealed that propylene glycol, distilled water, and oil could be used to create a phantom that mimics breast tissue permittivity well; however, the conductivity was not close enough. We used distilled water and propylene glycol as a starting point, but we needed to make changes to the phantom to match the dielectric properties to different breast tissues.

In previous work it was found the dielectric properties can be controlled by changing the amount of water [53], methanol, and ethanol [54]. We used these ideas and applied them to more complex mixtures. By varying the water contents one is able to control either conductivity or permittivity; however, both parameters are affected by adding materials, for these reasons more than two types of materials must be used to control the dielectric properties within a frequency spectrum. These facts lead us to the

belief that varying the materials from previous research [10] may result in a better match for both conductivity and permittivity. Before combining mixtures the dielectric properties of each of the materials were measured using Agilent 8570 high performance dielectric probe and Agilent E5071C network analyzer, the results of these measurements are shown in Figure 2. In this thesis, all permittivity graphs represent relative permittivity (ε_r).
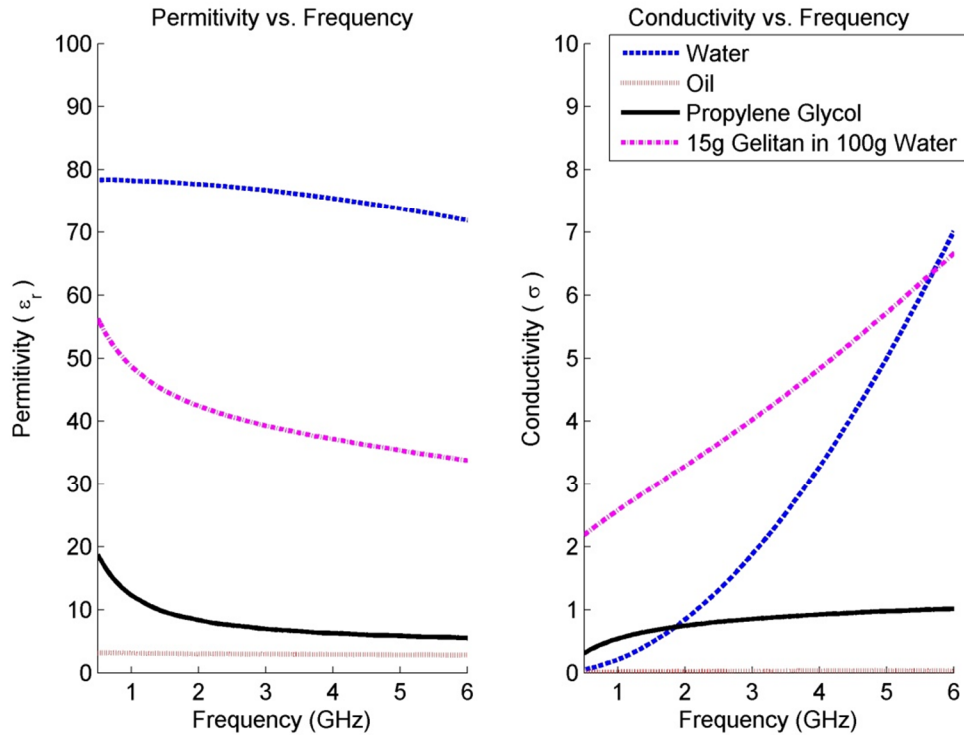
Figure 2: Independent measurements of different material types

From Figure 2 one can see that these materials have very different dielectric properties. It is expected that water will be used due to water's high permittivity for creating a phantom with high permittivity, while using the low conductivity of propylene glycol and oil allow for reduction of conductivity. This supports the original speculation that a mixture with low conductivity can be created from these materials.

3.3 Regression Analysis

Multivariable regression is a form of regression analysis that tests the response of one or more dependent properties based upon changes in several other independent properties [55], [56]. For this study the independent variables were considered to be the mass of each material used in the mixture: including water, oil, propylene-glycol, and gelatin. The dependent variables were considered to be conductivity and permittivity at discrete frequencies across the spectrum of interest. These dependent variables are chosen due to the dispersive nature of human tissue, i.e. the dielectric properties dependence on frequency [**7**], [23]. To begin regression the analysis a base data set is required. For this data set a group of sixteen mixtures were created by varying the mass of each material in the mixture. For each material used, bounds were set to provide the desired material properties. The regression equations are only valid within this range where data has been taken. The mixtures used to obtain the initial data set were derived from these extremes and are listed in Table 1. Each mixture in this set was measured across a frequency spectrum and the resulting data was compiled for multivariable regression analysis.

26

Table 1: Regression table

	Data sets used in regression analysis			
Test #	Water (g)	Oil (g)	Propylene Glycol (g)	Gelatin (g)
1	80	50	7	10
2	40	50	7	10
3	80	10	7	10
4	40	10	7	10
5	80	50	2	10
6	40	50	2	10
7	80	10	2	10
8	40	10	2	10
9	80	50	7	5
10	40	50	7	5
11	80	10	7	5
12	40	10	7	5
13	80	50	2	5
14	40	50	2	5
15	80	10	2	5
16	40	10	2	5

Regression analysis is a complex and repetitive task. Many software packages are available for these processes [57]. Minitab was chosen for analysis [57]. After processing the data, Minitab organized the data in a manner that was simple to understand.

```
Analysis of Variance for perm 1 ghz

Source          DF       SS        MS      F       P
Regression       4   35992.8   8998.21   41.29   0.000
Residual Error 235   51206.9    217.90
Total          239   87199.8

Regression Equation

perm 1 ghz=-31.0401 + 0.4212 (water) + 0.2749 (oil) + 2.5502 (prop) +
         0.2518 (gel)
```

Figure 3: Textual output from Minitab

When completing a regression analysis of a data set in Minitab, an output similar to one shown in

Figure 3 is generated. This output provides very important information regarding the regression data generated by Minitab, including: the dependent variable (e.g. permittivity at 1GHz: perm 1ghz), degrees of freedom (DF), mean squared (MS), sum of squares (SS), power of regression equation (P), location of the power in a normalized F distribution (F), residual error, and regression information [55]-[56]. This information provides some insight into how well the regression equation fits the data set. DF is the number of data points used to calculate the information minus one. SS is the sum of all of the data points squared; this is most useful in the residual error calculation due to the fact that the error can be positive or negative. MS is the mean squared of the residual error or regression data points [56] (High error due to a simple linear equation shows this equation is not adequate to model this data set in this case). F and P-values are directly related; F value is a part of a normalized probability distribution used to find the P-value of either a variable in the equation or the equation itself. The P-value describes the strength of the strength of a given hypothesis [56]. In this case we are testing the strength of each variable, and if this variable is necessary in the equation. Typically P-values of less than 0.05 are acceptable; in this case of this project we will be testing the significance of each variable. This is useful for eliminating variables from the equation.

In statistical tests, the P-values were zero for all cases (within the accuracy of the software), thus we accept that the relationship between the generated formulas and the actual data is very strong and that each variable is essential to the regression equation. However, after comparing these equations with previously measured mixtures, and analyzing residual errors (as listed in Table 1), through numerous trials, it was found that simple linear model, such as the one shown in

Figure 3, cannot accurately model the changes in this mixture. As recommended by William Navidi [55], the possibility of co-dependence of these materials was investigated. The results of this investigation conclusively showed that co-dependent regression variables were necessary for predicting a mixture's dielectric properties. The results of the regression equation for predicting the dielectric properties are shown in Figure 4. As one can notice, the equations did not perfectly predict the actual properties of the mixture. As more data was gathered, the equations became more accurate. The form of the co-dependent equation is shown in Equation (8).
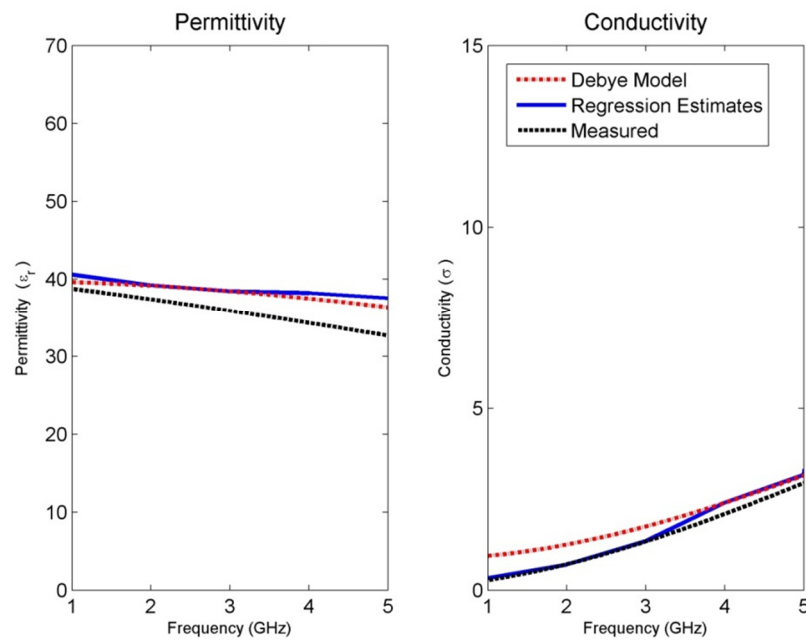
Figure 4: Depiction of regression model prediction for glandular phantom. The Debye model information was obtained from [12].

$$property = a_{constant} + a_1 m_{water} + a_2 m_{oil} + a_3 m_{prop} + a_4 m_{gel} + b_1 m_{water} m_{oil} + b_2 m_{water} m_{prop} +$$
$$b_3 m_{water} m_{gel} + b_4 m_{oil} m_{gel} + b_5 m_{oil} m_{prop} + b_6 m_{prop} m_{gel} + c_1 m_{water} m_{oil} m_{prop} +$$
$$c_2 m_{water} m_{oil} m_{gel} + c_3 m_{water} m_{prop} m_{gel} + c_3 m_{oil} m_{prop} m_{gel} + d_1 m_{water} m_{oil} m_{prop} m_{gel} + \text{constant}$$

$$(8)$$

$$40g < m_{water} < 80g$$
$$10g < m_{oil} < 50g$$
$$2g < m_{prop} < 7g$$
$$5g < m_{gel} < 10g$$

where a_i, b_i, c_i, and d_i are the regression coefficients given by regression analysis. m_{water}, m_{oil}, m_{prop}, and m_{gel} are the masses for water, oil, propylene glycol and gelatin, respectively. Equation (8) also provides the bounds for each material. These bounds are set based on to the range for which data has been taken. This range was determined through experiments performed previous to data collection. When the materials are outside of the given ranges the physical properties of the mixture begins to deviate from the desirable values, i.e. the mixture may become either fluid or physically too viscous to mix.

For this study, MATLAB [58] was used to process the regression equations and make predictions for various mixtures. Predictions were made by varying the amount of each material in the mixture, within the limits given in Equation (8), and calculating the dielectric properties using the regression equation. Invalid cases requiring negative mass or extreme amounts of each material were omitted from the solution provided by MATLAB. Many mixtures were considered and processed. For each mixture the amount of each of four main substances varied within the acceptable region as shown in Equation (8). The predicted permittivity and conductivity of each mixture at different frequencies were subtracted from the desired ones given by the Debye model [23] and the results

were recorded in an error matrix. The error was minimized by changing the amount of each four main substances. The mixture that provides minimum error was chosen.

3.3.1 Results of Multiple Iterations

Regression based design process is an iterative process; as more mixtures are created, and more data sets are collected, better regression models are obtained. After three iterations, the regression equation became substantially different from the initial equation. Different types of tissue phantoms (fat, transitional, fiber glandular, and skin tissues) required different number of trials; however, each trial for the four tissue types had the same data sets, The results for each of these trials are plotted in Figure 5-Figure 8, for fat, fiber glandular, transitional, and skin tissues, respectively. Acceptable ranges for each tissue type are shown with different background colors and shades. These correspond to the measured tissue properties in [7], [23]. One can see how, in general, the error decreases for each trial. As the regression process progressed the mixtures properties became closer to the desired properties. Figure 9 shows the measurement results of the selected tissue mimicking phantoms. In most cases the latest trial is the most accurate one. For the selected phantoms, the mass of different materials including formalin and surfactant for each tissue phantom are given in Table 2. Since formalin and surfactant were in small amounts, their effects on the dielectric properties were ignored and were not used as variables in the regression model. For each phantom 9 measurements were performed. The standard deviation (STD) at each frequency and for each phantom was calculated. The average of standard deviation for relative permittivity and conductivity over the frequency range of 0.5-1GHz for the selected phantoms (the same as those shown in Figure 9) are shown in Table 3.

31
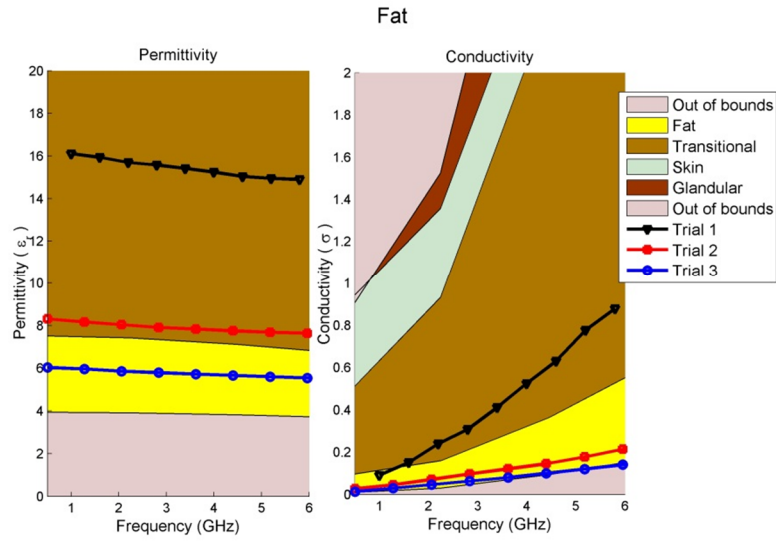
Figure 5: Regression results for fat phantom
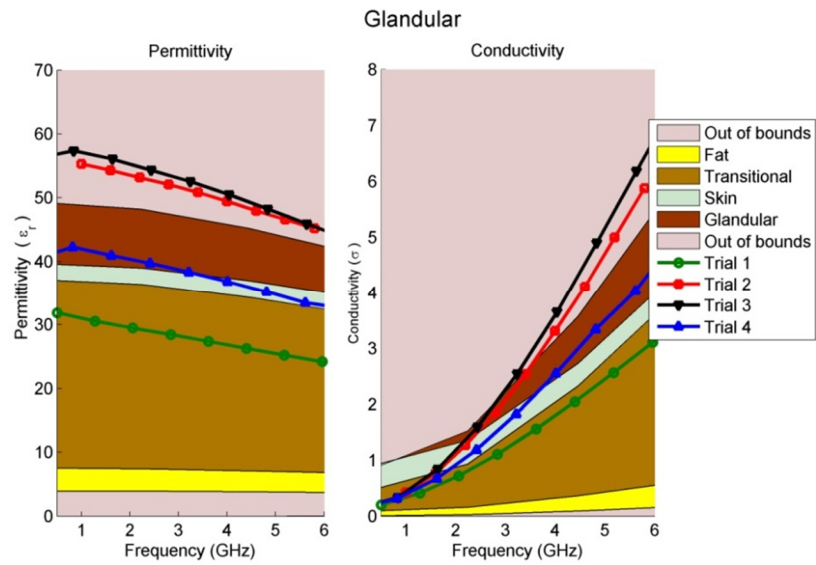
Figure 6: Regression results for fiberglandular phantom
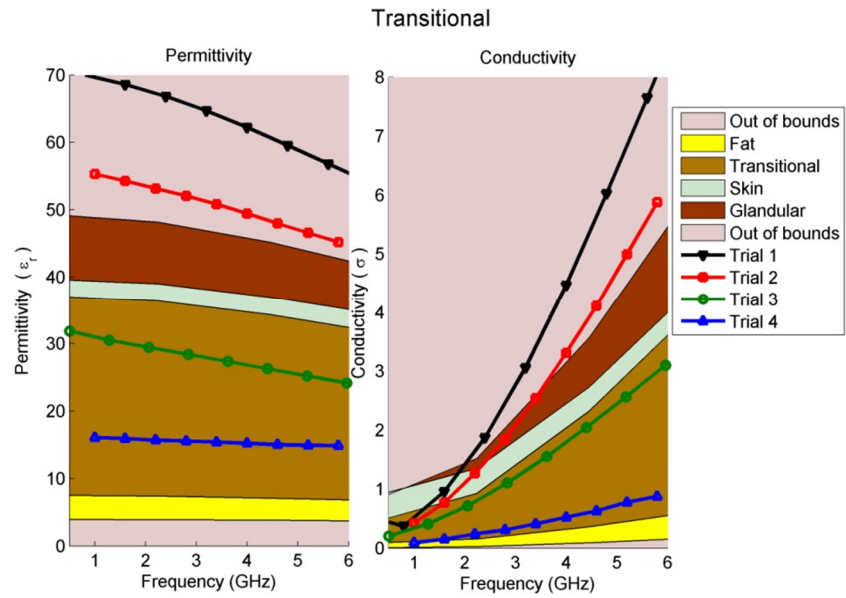
Figure 7: Regression results for transitional phantom
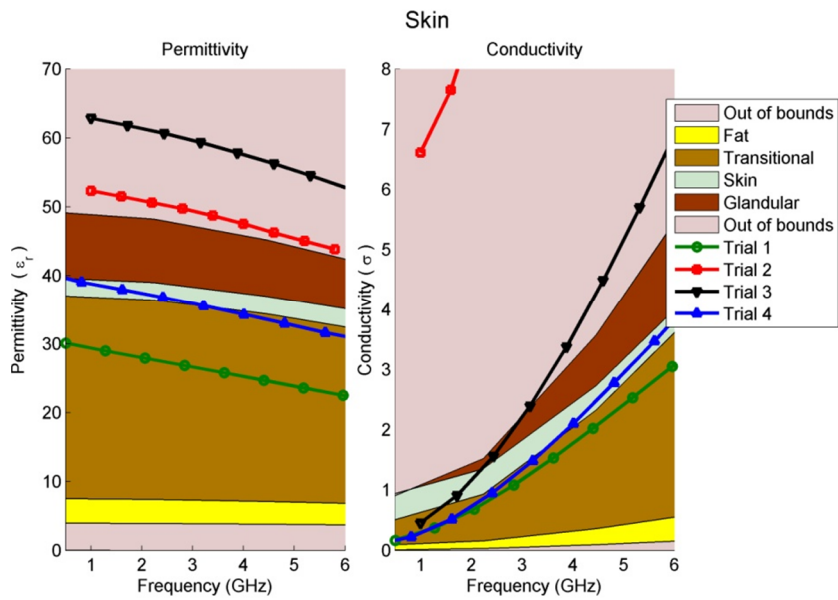
Figure 8: Regression results for skin phantom
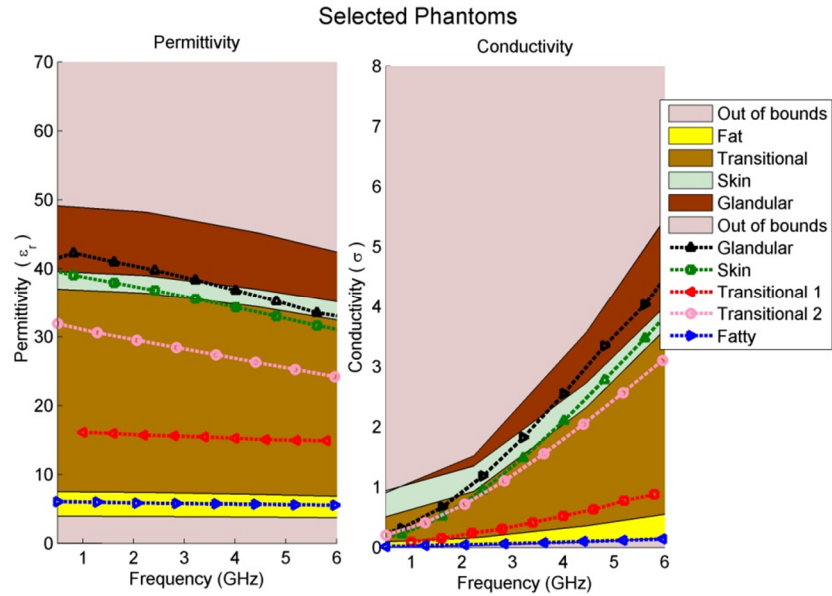
Figure 9: Final results for the selected phantom

Table 2: Mixture recipes (amounts in grams)

	Phantom Type			
Material	**Skin**	**Fiberglandular**	**Transitional**	**Fatty**
Distilled Water	80.00	80.00	40.00	40.00
Safflower Oil	14.00	21.00	13.00	39.00
Propylene Glycol	7.00	7.00	5.88	2.00
200 Bloom Calf-Skin Gelatin	5.88	5.00	5.00	7.00
Formalin	0.30	0.30	0.30	0.30
Surfactant	0.30	0.30	0.30	0.30

Table 3: Average of Standard deviation (STD) for selected phantoms shown in Figure 9 from 1-6 GHz.

Phantom Type	**Average of STD for ε_r**	**Average of STD for σ**
Fat	2.015	0.056
Transitional 1	3.372	0.252
Transitional 2	0.312	0.030
Skin	3.921	0.931
Glandular	7.029	0.478

3.4 Error Analysis

If the dielectric properties were within the acceptable range of each tissue the error was considered to be zero. The error for each tissue phantom was calculated across the entire frequency spectrum, using Equation (9). The error versus frequency for each

tissue phantom is shown in Figure 10. The average error over the frequency band is calculated and the results are shown in Table 4

Table 4: The average and standard deviation of error of different phantoms

	Average		Standard Deviation	
	Permittivity	Conductivity	Permittivity	Conductivity
Fatty Tissue	4.40%	0.02%	0.0570	0.1126
Skin	7.18%	6.32%	0.1421	0.0389
Fiberglandular Tissue	2.99%	11.74%	0.1160	0.0822
Transitional Tissue 1	0.16%	0.00%	0.0000	0.0000
Transitional Tissue 2	0.00%	0.00%	0.0077	0.0000

$$Error_\varepsilon = \sqrt{\frac{\left(\varepsilon_{Debye} - \varepsilon_{Regression}\right)^2}{\varepsilon_{Regression}^2}}$$

$$Error_\sigma = \sqrt{\frac{\left(\sigma_{Debye} - \sigma_{Regression}\right)^2}{\sigma_{Regression}^2}}$$

(9)

ε =Permittivity

σ =Conductivity
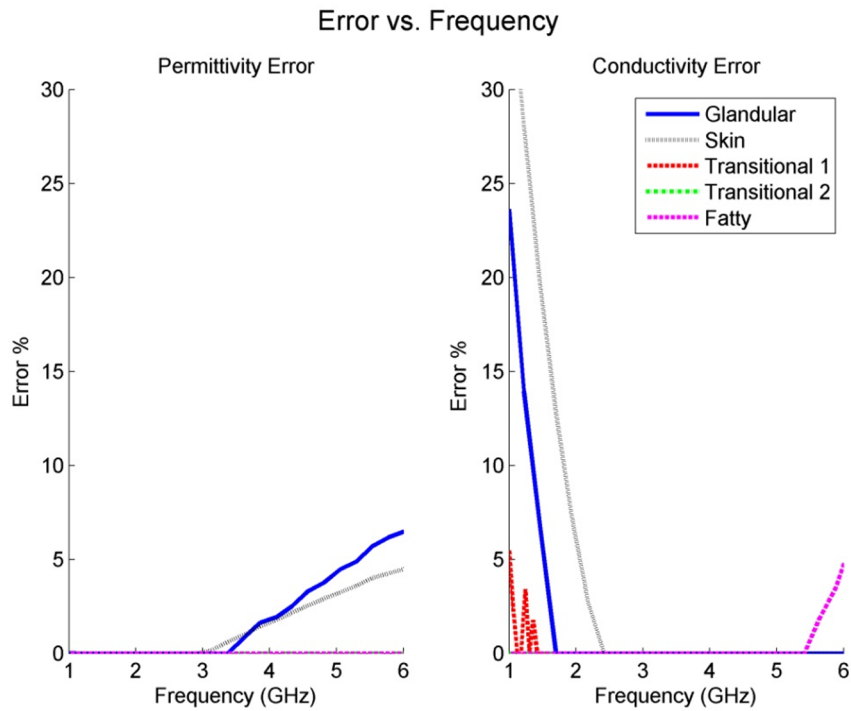
Figure 10: Error for each tissue mimicking phantom

Except for a few frequencies, the final phantom mimics the dielectric properties of breast tissues within 10%.

3.5 Procedure

To produce homogeneous mixture each material was measured with amounts prescribed in Table 2. A double boiler was used for heating and a container of ice water was used for cooling the mixtures, when needed. The first step was to mix the measured amount of distilled water with propylene glycol in a container to be placed in the double boiler. Then the temperature of the mixture was raised to $50°C$. After the water and propylene glycol reached $50°C$ the Calf Bloom gelatin was added and mixed in until it is completely dissolved. The result was a clear with a yellow color. While the gelatin was dissolving, the surfactant and formalin were added to the oil and was mixed with the

heated solution. Then the solution of water propylene glycol and gelatin was removed from the double boiler. At this point the remaining ingredients were added to the water and propylene glycol.

The mixture was continuously stirred until it cooled. After it cooled outside of the double boiler it was placed in the ice bath to cool further. Once it was in the ice bath, stirring was continued until the mixture reached 30°C. One should be careful not to stir too vigorously otherwise air bubbles will appear in the mixture and change its dielectric properties. Once the mixture reached 25°C it was poured into containers for molding, and then, refrigerated overnight.

3.5.1 Heterogeneous Phantom

To accurately assess the microwave imaging techniques, the object of interest must be of a heterogeneous nature. In this project a simple layered phantom was created to show the ability to manufacture such a phantom. This phantom is constructed with layers as shown in Figure 10. The mixing process discussed previously was used to produce each tissue type in the phantom and each layer was constructed from the exterior inward to produce a solid object.
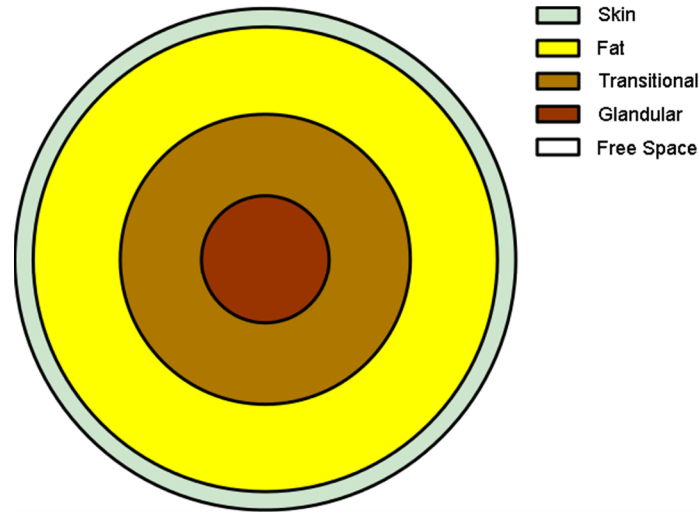
Figure 11: Structure of a heterogeneous phantom.

To create a model of the phantom shown in Figure 11, several cylindrical molds were required. First a large 6 inch diameter PVC pipe was sealed and used to produce a mold for the exterior. Then, a 5 inch diameter PVC pipe was used to form the inner wall for the skin layer. The inner concentric cylinder was removed after the skin phantom was solidified. The mixture for the skin type phantom was then poured and left to cool. After carefully removing the 5 inch diameter PVC pipe, a 3 inch diameter PVC pipe was placed in the middle and fat phantom was poured. The inner cylinder was removed and then a 1.5 inch diameter pipe was placed in the middle of the phantom to make the mold for the transitional phantom. After removing the final pipe the glandular phantom mixture was poured. The molds used for making this phantom are shown in Figure 12 and the final heterogeneous phantom is shown in Figure 13. Food coloring was added to show the different layers in the phantom.

Figure 12: Cylinders used to mold the phantom.

Figure 13: Heterogeneous phantom.
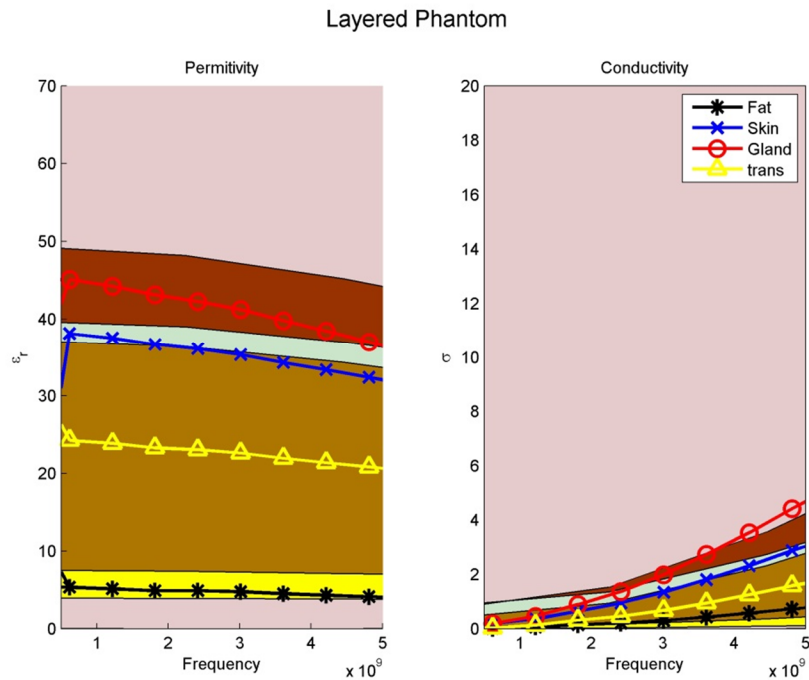
Figure 14: Dielectric properties measurements of each layer for the phantom.

The dielectric properties of each layer of the heterogeneous phantom were then measured. The measurements for the material of each type are shown in Figure 13.

3.6 Phantom Life Study

When using a phantom for benchmarking, it is important to understand how time, humidity and temperature affect the phantom properties and when the phantom is no longer usefully accurately mimics the tissue. For this reason several measurements of the dielectric properties were taken over the period of a week to better understand the behavior of the proposed phantom mixture over time. The results reported here are only from our initial study. More measurements are required to confirm the repeatability of the results. In addition the changes in dielectric properties when they are formed in a heterogeneous phantom and in contact with different layers should be studied.

Our hypothesis was that as the phantom ages, due to evaporation the water content decreases. This should cause a drop in the in permittivity over time. This change is inevitable, but to slow the evaporation two different storage techniques were tested: storing in low temperature, keeping the phantom in a closed container. Four identical phantoms were needed to start the study. The identical mixtures were obtained by creating one large mixture then dividing these into four different pieces for testing. Different methods of storage produced strikingly different results as depicted in Figure 15-Figure 18.
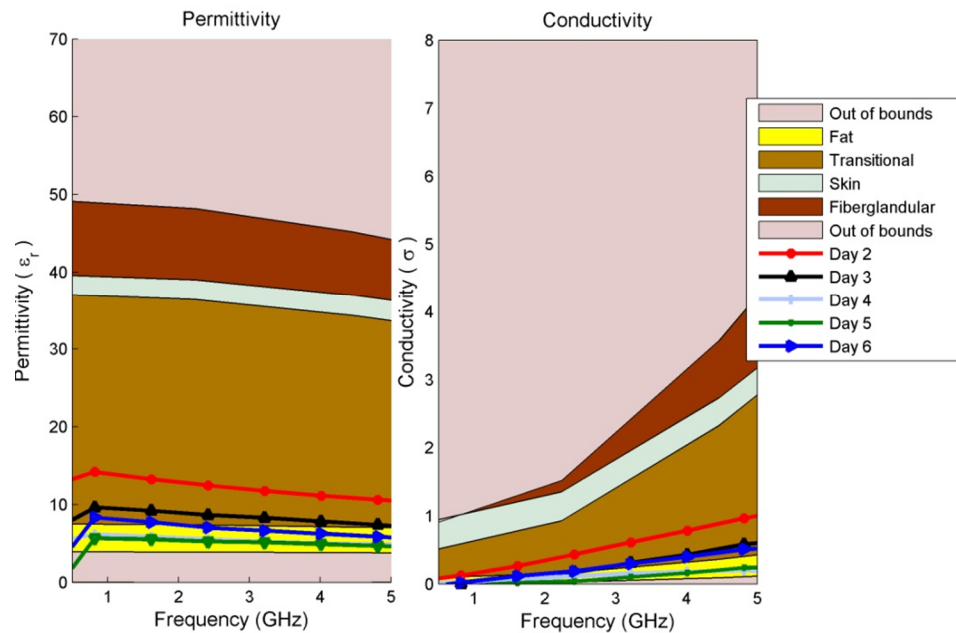
Figure 15: Transitional phantom kept in an open container at a low temperature
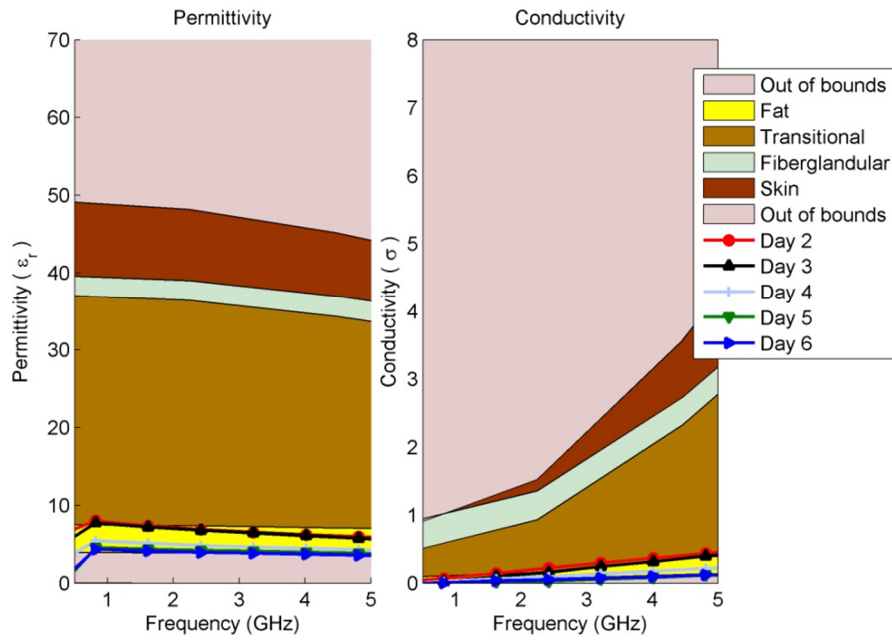
Figure 16: Transitional phantom kept in an open container at room temperature
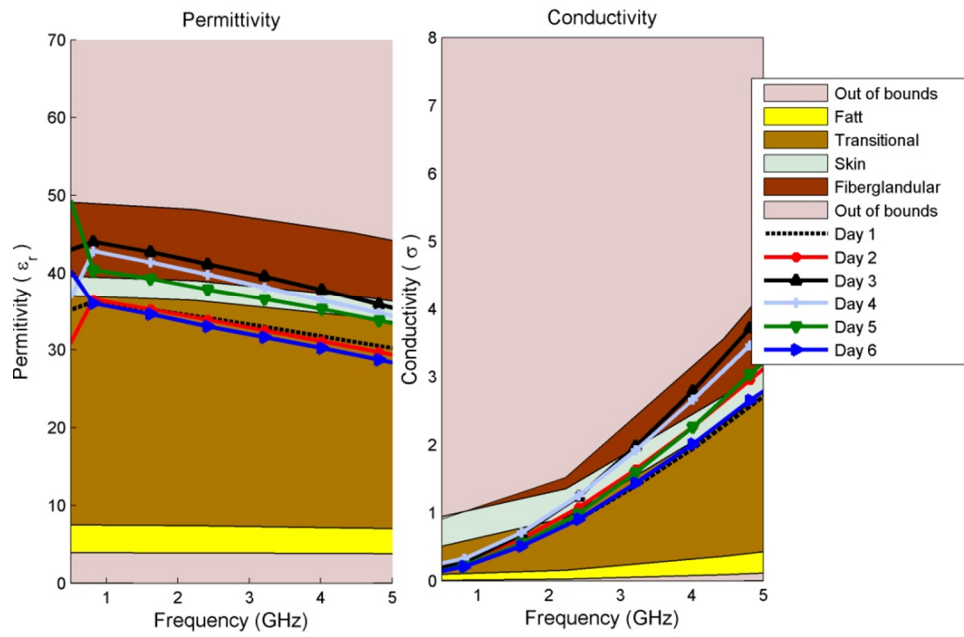
Figure 17: Transitional phantom kept in a sealed container at a low temperature
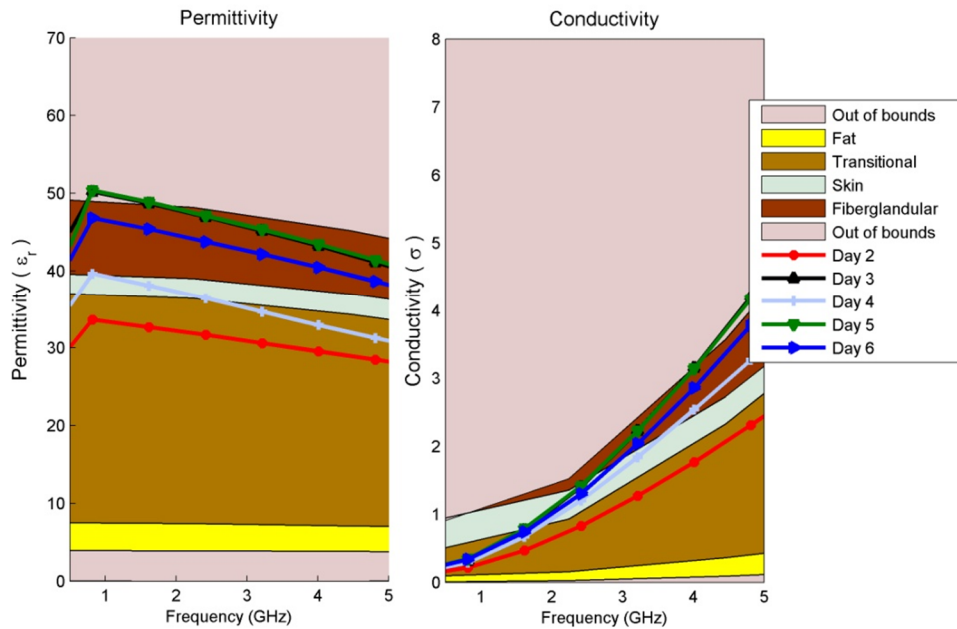
Figure 18: Transitional material kept in a sealed container at a room temperature

As time passed the permittivity of each sample decreased, as it was expected. Additionally, we found that if the material is placed in a sealed container the dielectric properties can change dramatically, this could be due to a change in partial pressure, removing some gas from the mixture and thereby causing the permittivity to rise. This phenomenon can be observed by comparing Figure 15 with Figure 17, as well as Figure 16 with Figure 18.

In conclusion, the dielectric properties seem more stable if the phantom is kept in a refrigerator, but not in a vacuum container. It should be noted that the phantom properties show substantial changes with respect to temperature, before using a phantom it is important to allow it to return to the room temperature. Under these conditions it appears that this phantom should be useful for up to 5 days.

3.7 Summary

We proposed a systematic approach to building tissue phantoms based on regression models. This process was used to form a mixture that adequately mimics different breast tissues with respect to their dielectric properties. This resulting phantom is made of a mixture that can be molded with many traditional molding techniques. By using a combination of molding techniques, one can adequately represent the physical and electrical properties of human breast. The results shown in this chapter are based on the available breast tissue dielectric properties from *ex vivo* measurements; therefore, the comparison is performed at room temperature. As a future study the phantom behavior at higher temperature (closer to body temperature) should be compared with *in vivo* tissue properties, once they become available. To provide information regarding the *in vivo*, the following chapter will discuss the design of a sensor for *in vivo* measurements.

CHAPTER 4: DIELECTRIC PROPERTIES PROBE DEVELOPMENT

None of the previous studies on the dielectric properties of human tissues [5]-[7] have adequately addressed the possible changes in the dielectric properties of tissues after excision. It has been hypothesized that when the tissues are excised, they lose blood and water during the removal process and change temperature [17], [20], [22]. Some researchers have tried to address the *in vivo* approximation by taking measurement during surgery or by minimizing the time from excision to measurement [59]. To adequately assess these changes, measurements need to be taken with the embedded probe. A truly implantable probe provides a means for investigations of properties of tissues under close to normal conditions. Currently most of dielectric properties measurement techniques are based on open ended probe that requires the use of a VNA or similar large equipment [5]-[7]. This chapter describes the investigation and experimentation into *in vivo* dielectric properties measurement technique that is wireless. For our purposes, this device should generate its own signal for measuring the dielectric properties at the desired frequency. This device should also include a wireless link for data transmission, to be processed later. With a wireless implantable dielectric sensor, a large amount of data can be collected and continuously dielectric measurements can be performed to follow the cancer growth.

4.1.1 Implanted Electronics in Biological Environments

In the past, many sensors have been proposed to be implanted in biological environments for research or treatment. These devices have been used to measure a variety of biological conditions including pH, pressure, and temperature [28]-[32]. Some of them were used in animal studies. Most of these devices are capacitive sensor. In a capacitive sensor the changes in the capacitance are measured and the property in question is calculated. Similar techniques can be used to measure dielectric properties of a tissue contacting the sensor. In the following section changes of capacitance with respect to the dielectric constant of the covering layer at various frequencies and calculations of permittivities are discussed.

4.1.2 Capacitive Dielectric Properties Sensor

It is well known that the capacitance of a parallel plate capacitor is directly related to the permittivity of the material between the plates in the capacitor [60]. In a similar way, dielectric properties of tissue placed on a flattened finger capacitor can be measured by measuring the changes in capacitance. To test this hypothesis several model capacitors were simulated by Ansoft Designer [61]. These capacitors were subjected to the simulation model shown in Figure 19. In this model a substrate was placed under the capacitor and a layer of simulated tissue was placed on the face of the capacitor. The thickness of the tissue was varied to determine the sensitivity of the capacitor. The size of the capacitor was also varied to assess the size requirement for this type of sensor.
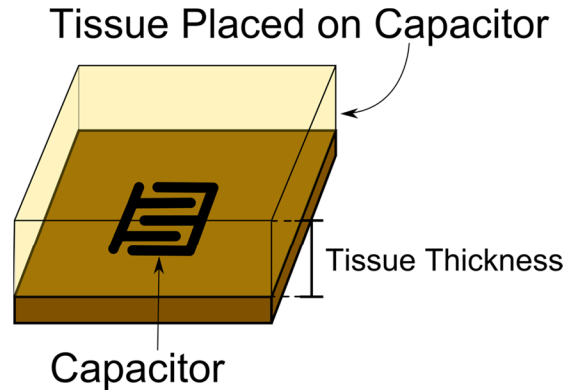
Figure 19: To adequately test the capacitance of the designed finger capacitor, the capacitor was constructed on a substrate, while several simulated tissues were placed on top of the capacitor. The thicknesses of these tissues were varied during the simulation to assess the sensitivity of the capacitor.

4.1.3 Simulation of Several Capacitors

To gain a better understanding of the size required for the capacitors, eight capacitors were simulated with various sizes. To assess the capacitors adequately the number of fingers and width of the capacitor was varied. The capacitors were simulated with respect to the model shown in Figure 20. The capacitors conform to a measurement standard shown in Figure 21 and the values in Table 3.
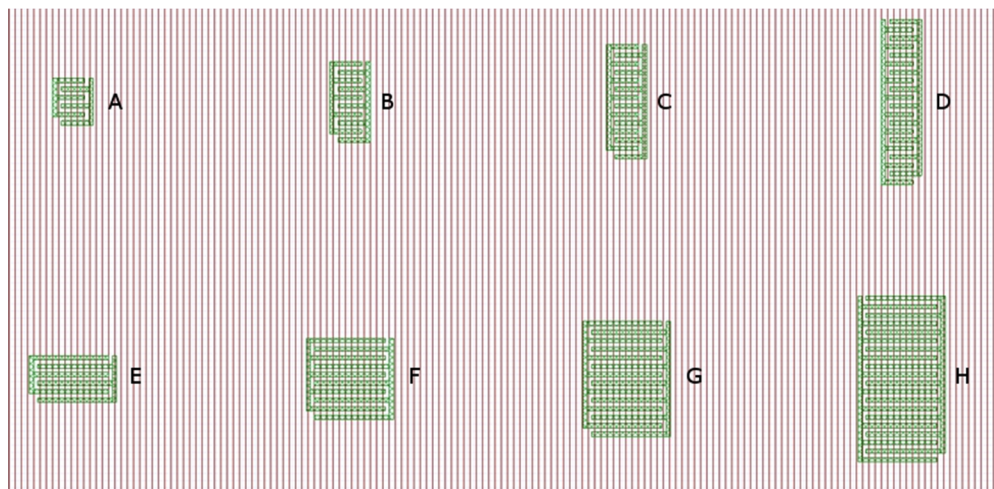
Figure 20: A depiction of 8 simulated finger capacitors. These capacitors were modeled with tissue as shown in Figure 19.
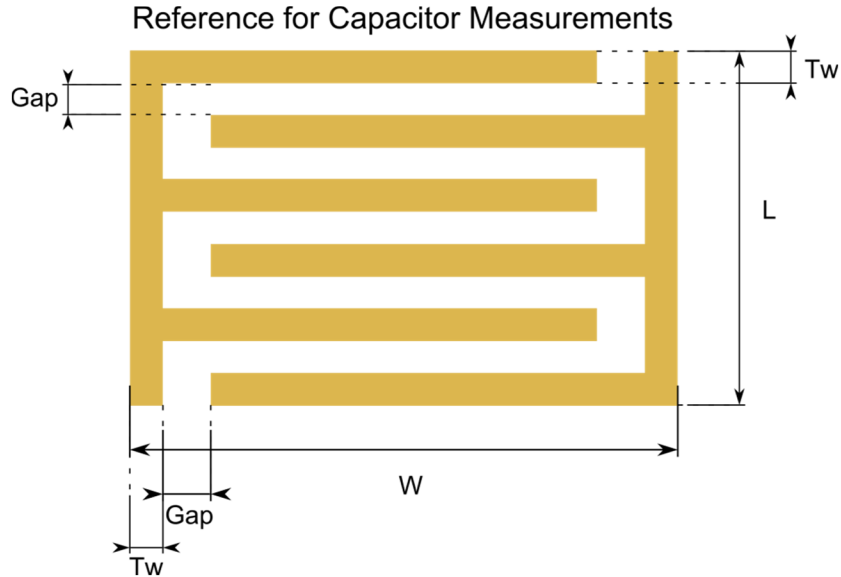
Figure 21: A depiction of the measurement locations for the capacitors in Figure 20

Table 3: A table of the measurement specification for the capacitors depicted in Figure 20. The dimensions are given in mm and with respect to Figure 21.

	Capacitor Label							
	A	B	C	D	E	F	G	H
# Fingers	6	10	14	20	6	10	14	20
W	1.450	1.450	1.450	1.450	3.160	3.160	3.160	3.160
L	1.675	2.900	4.110	5.000	1.675	2.900	4.100	5.040
Tw	0.152	0.152	0.152	0.152	0.152	0.152	0.152	0.152
Gap	0.152	0.152	0.152	0.152	0.152	0.152	0.152	0.152

The capacitance for each of these capacitors with a dielectric layer was placed on the top surface was evaluated. The dielectric properties of the dielectric slab were chosen to model different tissue types [5]-[7]. The intent of this study was to find the smallest size capacitor that provides enough sensitivity to measure the dielectric constant of top layer. All of the capacitors shown in Figure 20 exhibit a substantial change in the capacitance when different dielectric slabs are placed on top of them. The result of the simulation for the capacitor A is shown below in Figure 22.

Various Tissues Placed Upon Capacitor A
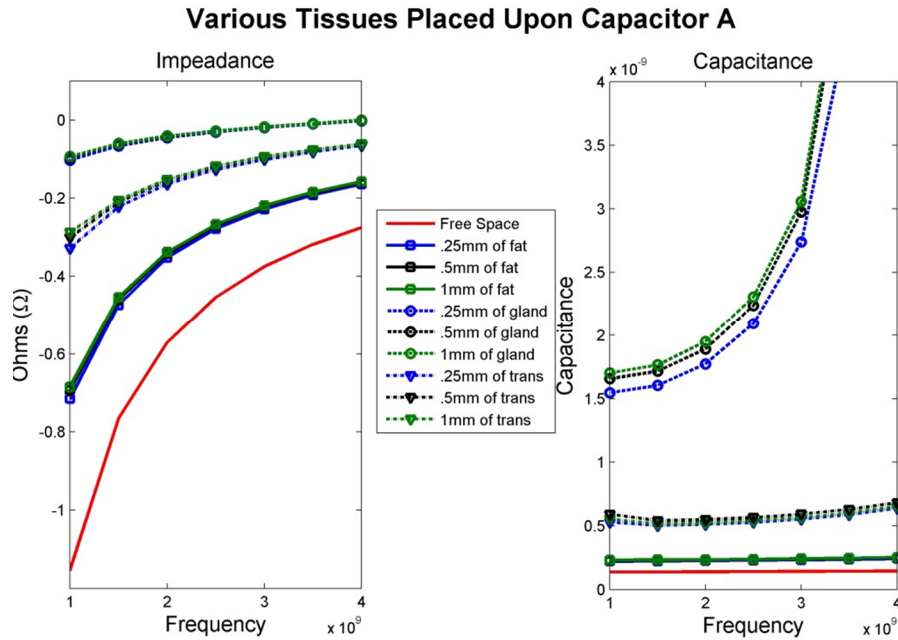
Figure 22: Simulation results for the capacitor A shown in Figure 20. The capacitor was subjected to the model shown in Figure 19.

With promising simulation results it is important to verify the results of simulation with physical measurements. The physical construction of the capacitors was designed to conform to the measurements in Table 3.

4.1.4 Initial Measurements

To assess the accuracy of the simulation, the simulated capacitors were constructed on a printed circuit board, shown in Figure 23. These capacitors were then measured by an Agilent 4284A Precision LCR meter at 1MHz. Simulation results were then compared to the physical measurements. The results of the measurement closely matched the simulations at this frequency, as shown in Table 4. With the promising changes in dielectric properties, a method for measuring these changes must be investigated. During both the simulation and the initial measurements no ground plane was used.

49
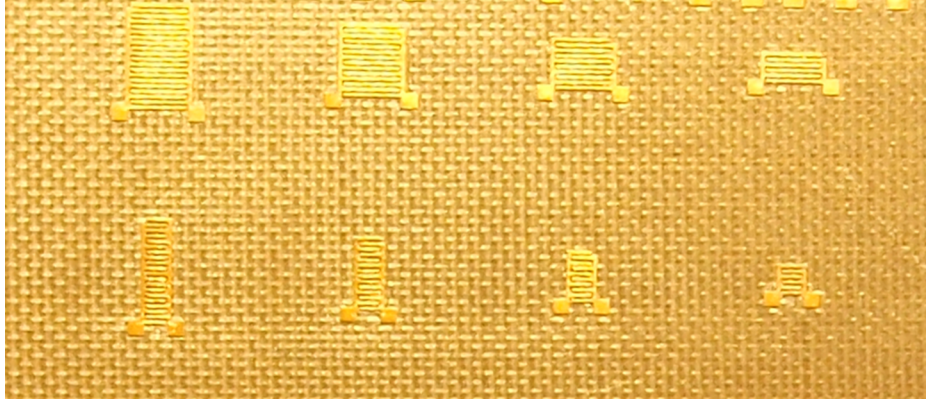
Figure 23: Fabricated capacitors for comparison with the simulation model. These capacitors were measured with an LRC meter and then compared with the simulation results in Table 4.

Table 4: 1 MHz simulation data compared measurements of the physically realized capacitors shown in Figure 23 measured with a precisions LRC meter.

	C1 (pF)	C2 (pF)	C3 (pF)	C4 (pF)	C5 (pF)	C6 (pF)	C7 (pF)	C8 (pF)
Measurement	0.041	0.06	0.138	0.191	0.568	0.42	0.236	NA
Simulation	0.039	0.058	0.131	0.189	0.550	0.41	0.231	0.059

4.1.5 Measuring Capacitance Changes

Several different methods for measuring capacitance were investigated before building a prototype sensor. Four different techniques for measuring capacitance changes are discussed in this section: capacitive bridges, capacitive voltage divider, resistive voltage divider, and LC oscillator. The most precise method to measure impedance is through a capacitive bridge, this method uses a π network to measure the real and imaginary impedance of a component. A second method is the use of a resistive or capacitive voltage divider. This method does not provide the accuracy of the bridge measurement process, but has fewer parts. The final method is the use of an LC oscillator. This method uses the oscillation frequency of the circuit to determine the capacitance of the component.

Wheatstone-Bridge Capacitive Measurements

The Wheatstone bridge is a resistive capacitive measurement technique. The Wheatstone bridge circuit is depicted in Figure 24. This measurement method works by changing the values of capacitor C5 and resistor R5 until the current that passes through these parts is minimized. Once no current flows through the resistor and capacitor, the resistance and capacitance is recorded, these values are then used to calculate the capacitance and resistance of the unknown load, R1 and C1. The number of elements needed for this method is its major negative factor. This method requires a frequency generator, digitally controlled capacitor, digitally controlled resistor, and microcontroller to dynamically balance the circuit. Each of these parts increases the overall foot-print of the device. The size and power consumption makes this measurement technique impractical for the purpose of implanted capacitive measurements.
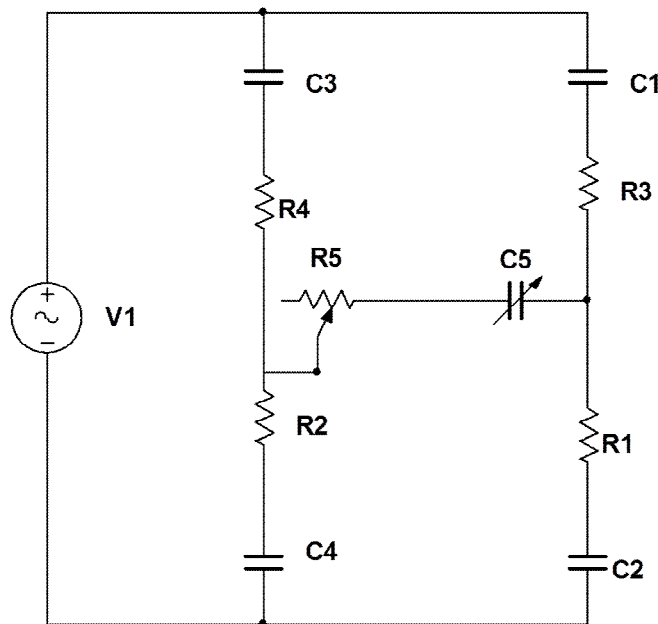
Figure 24: Bridge measurement technique.

Capacitive Voltage Divider

A capacitive voltage divider uses two capacitors in series and a radio frequency voltage source to measure the impedance magnitude of the unknown load. The alternating current source will generate a voltage across the capacitor that can be measured, as shown in Figure 25. The calculations for measuring capacitance in this manner are much simpler than in the Wheatstone bridge method. This method still requires an oscillator at the desired measurement frequency. For data acquisition and processing a microprocessor or other interpreting device is required. This technique requires fewer parts then the Wheatstone bridge technique, however, the specificity and accuracy is considered to be less than the accuracy of the Wheatstone bridge method.
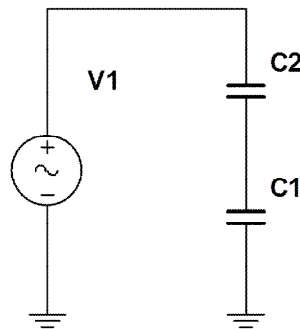
Figure 25: Capacitive voltage divider circuit.

Resistive Voltage Divider

The resistive voltage divider uses similar technology as the capacitive voltage divider, and provides similar information. The resistive voltage divider technique requires more computational; the frequency dependency still exists in the ratio of the voltages. This could cause an additional degree of inaccuracy. This method requires the same number of components as the capacitive voltage divider, but the use of a resistor does not

provide the simplicity of calculation that exists in the capacitive voltage divider. Figure 26 is a depiction of the measurement circuitry.
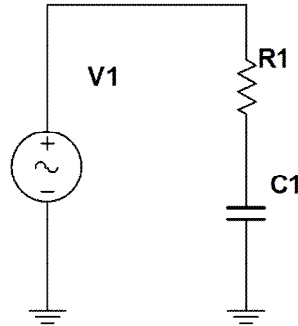
Figure 26: Resistive voltage divider that can be used to measure capacitance.

LC Oscillator Technique

With the LC oscillator technique an inductor capacitor resonant circuit is used to create a tunable oscillator. This oscillator will resonate at the frequency described by Equation (10) where the inductance, L, is known and the capacitance, C, is unknown. Using the known inductance in combination with the measured frequency the capacitance can be calculated. A spectrum analyzer might be used to detect the resonance frequency. This can be completed either at the source or upon transmission of the signal across a wireless link.

$$f = \frac{1}{LC}$$

f = frequency

L = Inductance   (10)

C = Capacitance

4.1.6 Measurement Technique Selection

An implantable sensor must be as small as possible; the need for a smaller system size implies the need for fewer components. All of the methods previously discussed

need a microcontroller, while this method does not need it, and there-by needs a smaller size. An additional benefit of this technique is the fact that the oscillator can be used to produce the carrier frequency. This method directly modulates the data onto the carrier wave. The dielectric constant of the material can be inferred by measuring the frequency shift.

4.2 Practical Realization

When moving from a theoretical investigation to a practical application several different techniques for creating the device must be investigated. In our first attempts at creating an LC oscillator, Hartley oscillator was considered due to its simple design. After investigating this method, it was decided that a more standard approach should be taken. Therefore, a small oscillator that uses an external LC tank circuit to set the oscillating frequency was chosen. It is important that the tank circuit should be external due to the fact that the "sensor" must be part of this circuit to allow for the measurement of the dielectric properties.

4.2.1 Hartley Oscillator

The Hartley oscillator is a simple single transistor oscillator. It needs a small number of parts that provides a small circuit size. This design, however, has some complications. The transistor used to amplify the oscillation must be able to operate at the desired frequency. In order to obtain operation between 500 MHz and 5GHz the transistor will need to be specially made. Gallium Arsenide Field Effect Transistor (GaAs FET) transistors are required to operate at frequencies in the Giga Hertz (GHz) range.

These transistors are very hard to find in surface mount package and are very sensitive to static electricity. A schematic for the Hartley oscillator is shown in Figure 27.
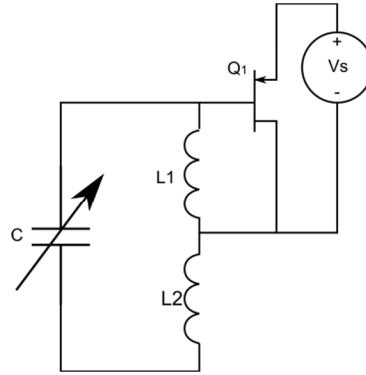
Figure 27: A simple Hartley oscillator. The variable capacitor represents the sensor capacitor.

This oscillator was constructed on a printed circuit board and assembled. An image of the assembled oscillator is shown in Figure 28. This circuit uses an external power source. The output signal is sent to the SMA connector. During the placement of the GaAs FET any static electricity can cause damage to it. The sensitivity of this component made this design not very successful. The values used to build the Hartley oscillator are given in Table 5.

Table 5: Parts list for the Hartley oscillator.

Part	Value
Q1	High Frequency GaAs FET
L1	6 nH
L2	21 nH
C	Capacitor A
Vs	3 V
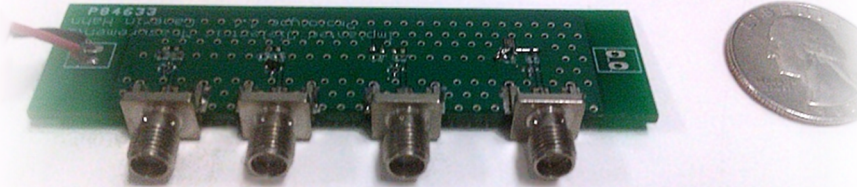
Figure 28: Original Hartley oscillator printed circuit board design. (4 sensors on board)

4.2.2 Standard ASIC Oscillator

After the problems encountered with constructing a Hartley oscillator a more conventional design approach was taken. This design uses typical "off the shelf" components to establish oscillation. Currently, there are few devices that allow the use of an external LC tank circuit. We chose MC100EL1648 voltage controlled oscillator (VCO). This VCO can operate up to 1 GHz, and more importantly, it incorporates an external LC tank circuit. The schematic of this oscillator is shown in Figure 29. This circuit was built and tested.
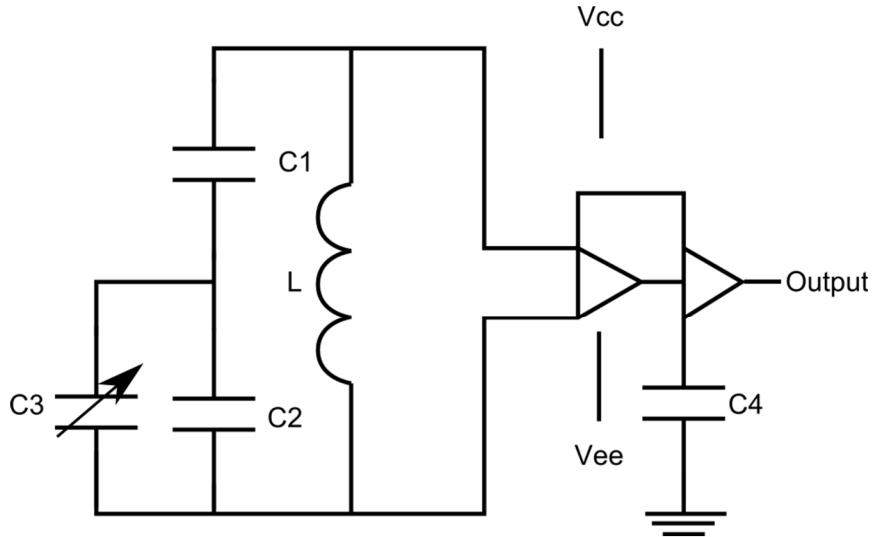
Figure 29: Circuit diagram for the oscillator built using a VCO. The variable capacitor is the sensor capacitor; the two fixed capacitors are used to adjust the center operation frequency as well as the sensitivity.

Table 6: Values for the components shown in Figure 29.

Label	Value
Vcc	1.5 V
Vee	-1.5 V
L	27 nH
C1	4 pF
C2	1 pF
C3	Capacitor A
C4	100 pF

The sensor was tested under laboratory conditions with components of the values shown in Table 6. It was attached to a spectrum analyzer via a 50 ohm low loss cable and to the dual voltage power supply. A small amount of water was placed on the sensor capacitor using a pipette. The frequency spectrum of the sensor was recorded from 400 MHz to 500 MHz. Different materials were placed in contact with the sensor capacitor and the measurements were repeated. To illustrate a typical frequency shift due to the dielectric placement on the sensor capacitor, the frequency spectrums for both water and air have been plotted in Figure 30. This sensor should be fully submersible.
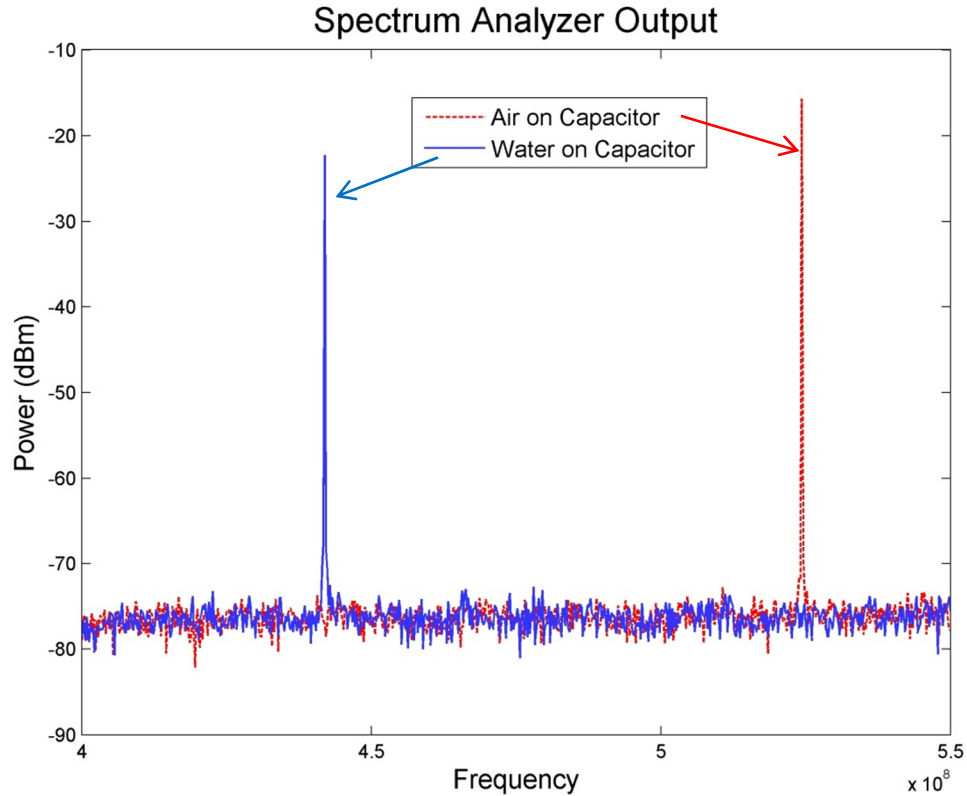
Figure 30: Measurements taken for a prototype probe. For the case of air the capacitive sensor was not exposed to a dielectric. For the case of water on the capacitor, water was applied with a pipette to the capacitor.

The second version of this design was constructed on a circuit board as shown in Figure 31. The changes were made so one side of the sensor could be sealed and the other side remain unmodified. The unmodified side contained the sensor capacitor. This capacitor must be in contact with the dielectric for a measureable change in capacitance to occur. First attempt for sealing the top side of the board was to use silicon rubber and placed it directly on the circuit elements. This caused changes in the capacitance of the lumped element capacitors and caused the sensor to stop functioning under any obtainable laboratory conditions. To allow the sensor to function properly, a cavity was placed around the surface mount components. The surface area of the package without the sensor capacitor was then covered by silicone. An image of the sealed sensor using a

free space cavity over the components is shown in Figure 32. This sensor was then tested in air, water, alcohol, oil, and mixtures of these materials. The dielectric properties of these mixtures were recorded and plotted against operational frequency of the oscillator, this information in shown in Figure 33.
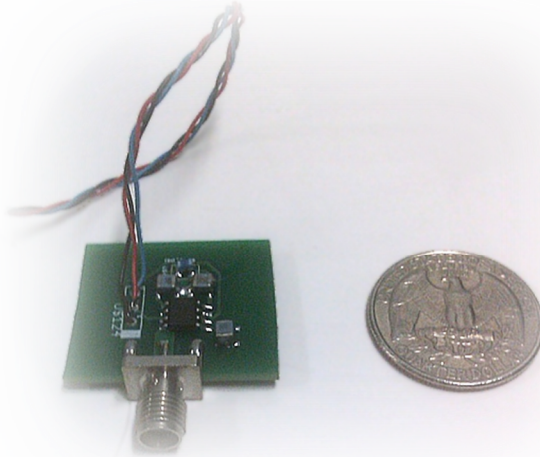
Figure 31: Second design constructed with a MC100EL1648 VCO.
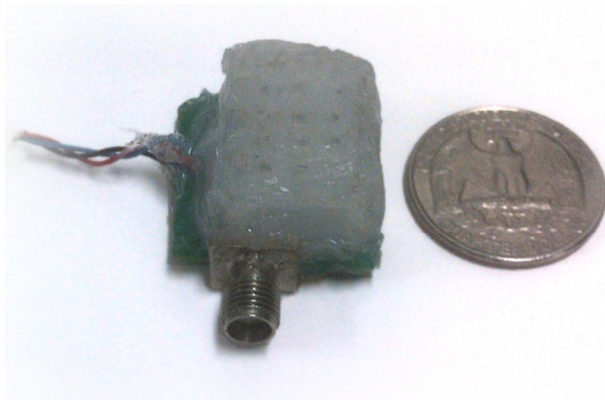
Figure 32: One prototype sensor sealed with silicone, a plastic shroud was used to provide an air gap above the sensor components.
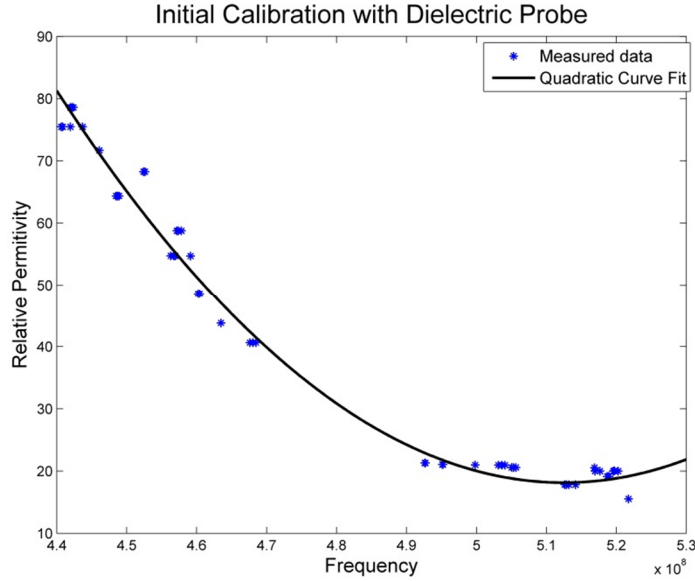
Figure 33: Frequency response of a prototype sensor to various dielectrics. The sensor was immersed in solutions of alcohol and water or oil and alcohol, the permittivity was recorded as well as the dielectric properties. Simple quadratic curve fitting was applied to find a trend.

After the regression process was completed, the data was shown to fit the form of Equation (11). Through the combination of this regression equation and the measured oscillation frequency of the implantable sensor, the dielectric properties of the material in contact with the sensor capacitor can be calculated.

$$\varepsilon_{measured} = -7.20\left(f_{measured} - 4.80*10^8\right) + 41.12$$
$$\varepsilon_{measured} = \text{Estimated permitivy of material on the sensor}$$
$$f_{measured} = \text{Frequency of oscilator during measurement}$$

(11)

Measuring at Multiple Frequencies

As with any oscillator, in the proposed oscillator harmonics are generated. These harmonics depend upon the capacitance of the LC tank. To verify this possible correlation a generic regression was calculated. For this regression both the permittivity and frequency were normalized according to Equations (12) and (13) respectively. The results are displayed in Figure 34.
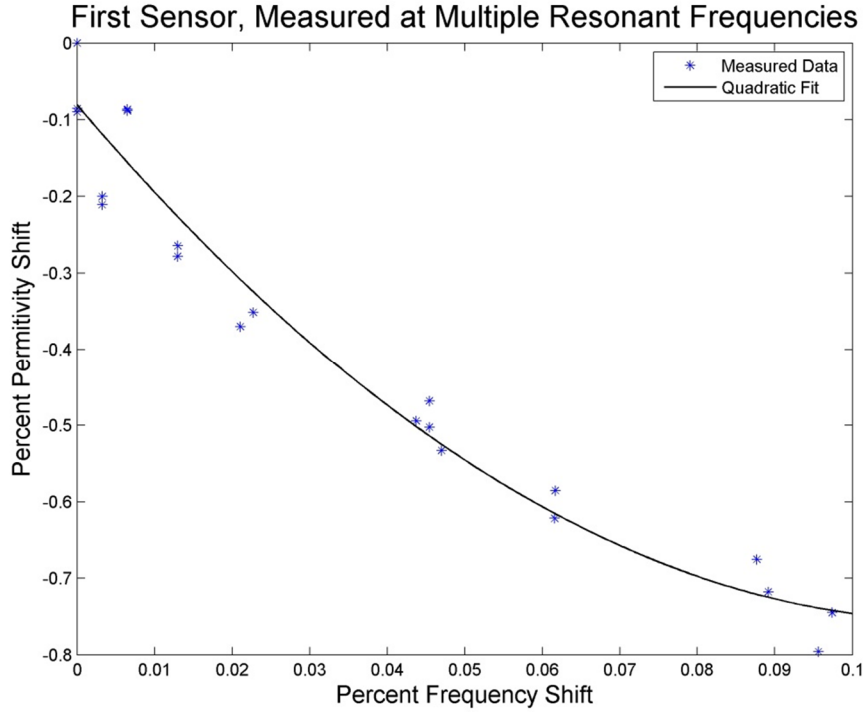
Figure 34: Measuring permittivity at multiple frequencies using first sensor. Percentage of permittivity shift was calculated using Equation (12). Percentage of frequency shift was calculated using Equation (13).

$$\varepsilon_{norm.} = \frac{\varepsilon_{water} - \varepsilon_{material}}{\varepsilon_{water}}$$

$\varepsilon_{norm.}$ = Normalized permittivity   (12)

ε_{water} = Permittivity of water

$\varepsilon_{material}$ = Permittivity of matieral

$$f_{norm} = \frac{f_{Water} - f_{Material}}{f_{Water}}$$

f_{norm} = Normalized Frequency   (13)

f_{Water} = Frequency of oscilaton for water

$f_{Material}$ = Frequency of oscilaton for material

$$\varepsilon_{norm} = A(f_{norm})^2 + B(f_{norm}) + C$$ (14)

Table 7: Coefficients of a curve fitting using generic regression equation in the form of Equation (14).

	A	B	C
Generic Regression Values	52.74	-11.93	0.08

4.2.3 Second Sensor Test

To confirm the results and test the sensitivity of the designed sensor, a second sensor was fabricated and tested. It was expected that this sensor would have different calibration curve, due to the fabrication differences. The same calibration method was used and the results are shown in Figure 35. The fitted curve coefficients for the second sensor are shown in Table 8. These values are calculated for regression Equation (14).
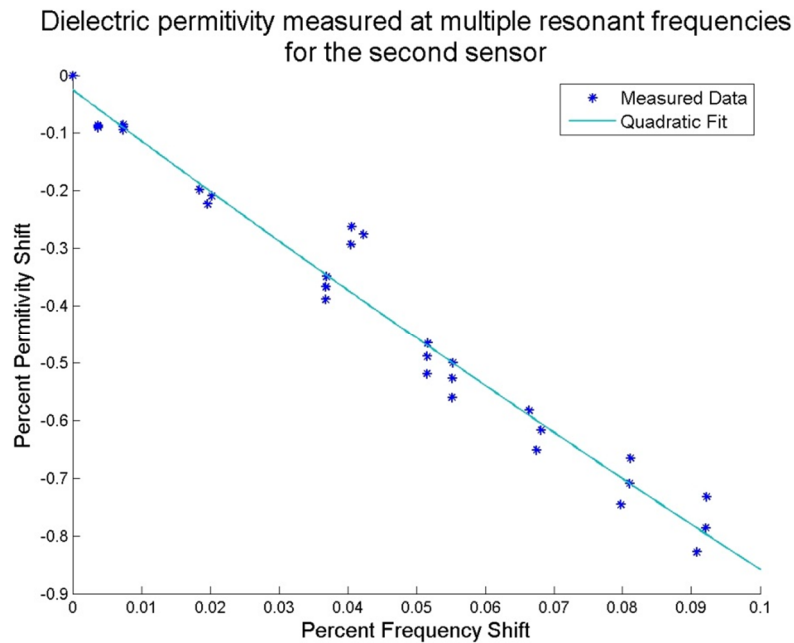
Figure 35: Plot of the calibration graph with the regression curve for second sensor. Percentage of frequency shift was calculated using Equation (13). Percentage of permittivity shift was calculated using Equation (12)

Table 8: Generic regression equation values for sensor two calibrations. These values are for a regression equation of the form of Equation (14)

	A	B	C
Curve Fitting Values	5.9059	-8.92	-.024

4.2.4 Measuring the Dielectric Properties

After completing the regression analysis for the first sensor, it was tested with four simple mixtures of isopropyl alcohol and water. The dielectric properties of these mixtures were measured with the Agilent 8570 high performance probe attached to the Agilent E5071C network analyzer, calibrated according to the specifications of the equipment. Tow measurements are compared in Table 9. The error is according to Equation (15).

Table 9: A comparison of the proposed capacitive sensor to a commercial dielectric properties probe measuring the dielectric properties of an unknown material. The capacitive probe used the generic regression equation.

Frequency (GHz)	Δf (MHz)	ε_r Measured with Capacitive Probe	ε_r Measured with Commercial probe	Error
0.498	38.1	27.1	26.6	2.22%
0.493	43.6	32.8	32.1	2.17%
0.478	58.6	49.3	52.6	6.31%
0.471	65.4	57.3	54.8	4.63%

$$Error = \left| \frac{\varepsilon_{Capacitive\,Method} - \varepsilon_{Commercial\,Method}}{\varepsilon_{Commercial\,Method}} \right|$$

$\varepsilon_{Capacitive\,Method}$ = Permittivity estimated by sensor

$\varepsilon_{Commercial\,Method}$ = Permittivity measured by commercial probe

(15)

4.2.5 Power Consumption

If this sensor can be used in a truly *in vivo* environment, the power consumption must be very low. It might need to operate using harvested energy. If it consumes more energy than could be harvested, it will not function. During operation of the probe, DC voltage and current measurements were taken. From these measurements the power

requirements for the probe was calculated. These values are shown in Table 10. We believe that with this very small power requirement, enough power can be harvested to allow for operation while implanted.

Table 10: Power Consumptions for the sensor.

	Voltage	Current	Power	Total Power
Sensor 1 Positive	1.49 V	0.01 mA	0.016mW	0.032mW
Sensor 1 Negative	-1.51 V	0.01 mA	0.016mW	
Sensor 2 Positive	1.49 V	0.01 mA	0.015mW	0.031mW
Sensor 2 Negative	-1.51 V	0.01 mA	0.016mW	

4.3 Conclusions

A method for measuring dielectric properties has been presented. This method uses very few parts and can be adapted for use as part of an *in vivo* dielectric sensor. For this sensor to become viable an antenna must be designed. Biocompatible packaging is required to use the senor for *in vivo* dielectric properties measurements.

CHAPTER 5: FUTURE WORK AND CONCLUSION

As this project moves forward, many considerations must be taken. For the phantom development aspects of this project, simplifying the regression equation and continually updating the phantom recipe to match the latest data regarding the dielectric properties of human tissue should be investigated. The dielectric property sensor requires substantial work before completion. This project should progress in several stages of research. This chapter will discuss the following: the development of the power management system, the power supply system, antenna design, bio-compatible packing and animal testing. When the sensor project is completed the phantom can be updated to match the tissue properties measured by the dielectric properties sensor.

5.1 Progression of Phantom Research

This thesis has discussed the process of designing a phantom based upon statistical modeling and simple regression analysis. This process is designed to provide the researcher a method to quickly and efficiently design a phantom to match a specific application. This project is not complete, however. At this point three different steps should be taken towards advancing the phantom design. The first step is simplifying the estimation process. Currently, the iterative solving process is very slow. The second step is adapting this phantom to match emerging *in vivo* tissue data on dielectric properties. The final step that should be taken is to use the phantom in different microwave imaging setups. These steps are explained in detail in this chapter.

5.1.1 Reevaluating the Regression Analysis

Currently, the regression equations used for the development of the phantom require a strenuous optimization process to find the appropriate mixture. As discussed earlier, the regression equations are calculated by considering the dielectric properties of the material a function of material content. With this assumption, the researcher must now optimize the mixture contents to match the dielectric properties of human tissue. It would be desirable to have an equation that directly calculates the mixture contents for a given dielectric properties curve. This will eliminate the inherent optimization required for the current method. Some considerations have to be taken when approaching this problem, including: bounding the material contents within a realizable range, statistical validity of regression model, and accounting for the co-dependence of the material masses.

5.1.2 Matching Emerging Dielectric Properties Studies

The strength of this design process for a dielectric phantom is the adaptability of the phantom. Many designs are based upon trial and error for finding a phantom with appropriate dielectric properties. These methods are not efficient and cannot quickly adapt to the changes in the data regarding the dielectric properties of tissue. The use of regression provides a quick and efficient way to adapt the dielectric properties of the phantom to the measured tissue properties. As new data becomes available including *in-vivo* properties, new phantoms should be developed using the same process.

5.1.3 Casting Method for the Phantom

This thesis presents only simple casting techniques for gelatin phantom. Ideally a more rigorous casting technique should be developed for more realistic phantom shapes. The more realistic phantoms should include heterogeneously scattered tissues to mimic different breast types such as: fatty, dense, scattered fiber glandular, dense fiber glandular, extremely fiber glandular.

5.1.4 Using the Developed Phantom in Microwave Imaging Setups

The goal is benchmarking a microwave imaging system. Therefore, this phantom should be used in several imaging systems, and image should be reconstructed using. By comparing the results of these measurements, researchers can deduce the pros and cons of each imaging system.

5.2 Dielectric Sensor Development

The proposed sensor is the first step toward development of a wireless implantable sensor. The design has to be completed by adding the energy harvesting unit. Energy harvesting can be done using radio frequency (RF) energy. A voltage regulation system also needs to be implemented to control the input power for the oscillator. For a wireless communication link a small antenna must be developed. This antenna has to be designed for the frequency band that the sensor operates on. RF power harvesting needs to be done at a different frequency and a second antenna has to be designed for this purpose. The completed sensor has to be packaged using biocompatible materials. The sensor can be then used in an animal study. The following is a discussion of the suggested steps.

5.2.1 Power Harvesting System

The sensor requires a power supply that can remotely obtain enough energy to power the sensor. At this point it is assumed that this power system will collect radiated energy and transfer it to DC power. The DC power needs to be regulated to provide constant voltage and enough power. To convert the RF energy to DC voltage, high frequency schottky didoes can be employed. These diodes can be arranged into any of the traditional voltage rectification techniques, providing DC power with a small footprint. As for the radiating power source, this system should conform to the Specific Absorption Rate (SAR) regulations. Along with this regulation, it is important to consider the effects of the chosen spectrum in terms of electromagnetic compatibility.

5.2.2 Voltage Regulation

After the power harvesting system is developed, a method of controlling the output voltage must be established. For the current design, this circuit must produce a steady output voltage of 1.5 volts. One of and simplest method to produce a steady output voltage is through the use of a Zener diode and a transistor. This will produce a simple linear voltage regulator. The circuit for a simple voltage regulator is shown in Figure 36.
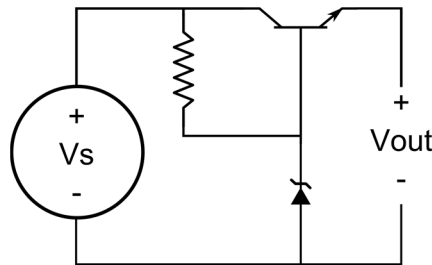
Figure 36: A simple Zener diode linear voltage regulator.

5.2.3 Antenna Design

Antenna design is a critical and challenging task. A dual frequency antenna might be considered to be used for both power harvesting and data transmission. However, this may not be practical. The possibility of interference between the higher power harvesting system, and the much lower power data transmission system may destroy the data being transmitted. Additionally, the energy harvesting antenna may require an antenna design to allow for maximum energy harvesting. This may result in utilizing the majority of the sensor surface for energy harvesting.

5.2.4 Biocompatible Packaging

Biocompatible packing is necessary for any implantable sensor. A vision of what that probe should look like is depicted in Figure 37. Ideally the sensor should be small enough to be implanted through injection.

(a)   (b)
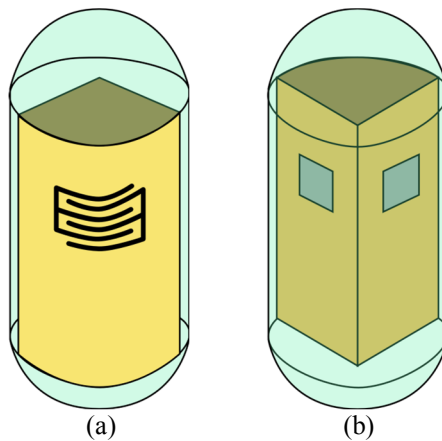
Figure 37: A depiction of the dielectric properties sensor. (a) sensor side, (b) antenna side

5.2.5 Animal Study

The goal is to utilize this sensor in an animal study. It is possible to grow cancer cells similar to human breast cancer in certain types of rats. Therefore, the sensor can be used to follow the cancer growth. This study will not only provide information about the dielectric properties of the cancerous tissues, but also the information about how the dielectric properties of developing tumors changes. The current vision for the dielectric properties measurement setup is depicted in Figure 38. In this depiction the sensor is implanted in an animal. An RF power signal provides energy through an antenna, and a second antenna is used to receive the data transmitted by the sensor using a spectrum analyzer. The frequency of oscillation received by the spectrum analyzer is compared with the calibration regression equation to calculate the permittivity of the tissue.
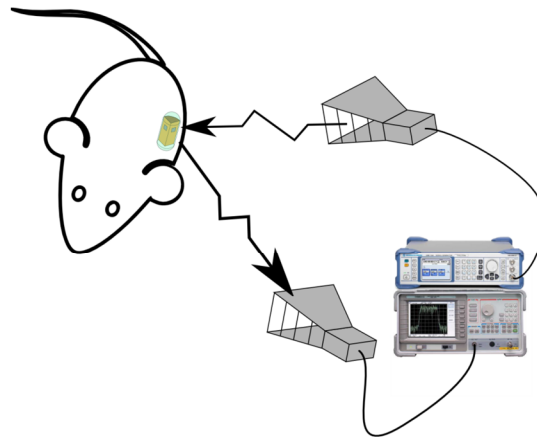
Figure 38: A possible setup for measuring the dielectric properties of tissue using an implantable sensor.

With the data *in vivo* dielectric properties from the animal study, a phantom should be developed using regression method. This phantom should be realistic to be used for benchmarking microwave imaging setups. Allowing microwave imaging researcher's access to a standard, up to date, and heterogeneous breast phantom would provide a simple method for comparing developing systems and algorithms.

70

5.3 Conclusion

This thesis has presented a method for developing a dielectric phantom systemically. Using this approach it is possible to simply adjust the phantom recipe as new information regarding the dielectric properties of the tissue emerge. To have a realistic phantom and more accurate imaging system, a truly *in vivo* study of dielectric properties needs to be completed. As a starting point, a sensor that can be used in a wireless measurement system was developed. This method employed a finger capacitor for sensing the dielectric properties of a material in contact with the sensor. This capacitor is then used as part of a capacitive inductive circuit to produce a sinusoidal wave. The frequency of oscillation of this wave is directly dependent upon the capacitance of the sensor and the permittivity of the tissue covering the capacitor. The frequency shift can be measured through a wireless link to by preform an *in vivo* measurement. In the future the sensor must be completed by adding antennas and an energy harvesting system. The results of *in vivo* measurements can be utilized to build a phantom with high accuracy for assessment of microwave imaging setups.

APPENDICIES

Appendix A

Regression Equation Function for Permittivity (MATLAB)

```
function [out]=perm_reg(water, oil, prop, gel)
freq=[1; 2; 3; 4; 5; 6]*10^9;
% The vector below  includes all of the possible codependence with respect
% to the 4 input values of water oil propylene glycol and gelatin in grams
inval=[water; oil; prop; gel; water*oil; water*prop; water*gel; oil*prop;
    oil*gel; prop*gel; water*oil*prop; water*oil*gel; water*prop*gel;
    oil*prop*gel; water*oil*prop*gel];
% the following is a regression equation for the frequency of 1 ghz
eq2 =[0.762 0.1578  3.4903  11.6028 0.0179  0.1131  -0.1129 -0.2312
    -0.0142   -0.3815 0.0001  -0.0024 -0.0127 0.01    0.0004];
% the following is a regression equation for the frequency of 1 ghz
eq4 =[0.7345   0.1561 3.4745 11.1626 0.0174 0.1097 -0.1084 -0.2248
    -0.0155  -0.3807 0  -0.0023 -0.0124 0.0096  0.0004];
% the following is a regression equation for the frequency of 1 ghz
eq6 =[0.7088   0.1581 3.4529 10.7431 0.0171 0.1061 -0.1044 -0.2195
    -0.0167  -0.3774 0  -0.0022 -0.0121 0.0093  0.0004];
% the following is a regression equation for the frequency of 1 ghz
eq8 =[0.677 0.1574  3.4229  10.2004 0.0165 0.1011  -0.0986 -0.2118
    -0.0182  -0.3717 0  -0.0021 -0.0116 0.0091  0.0004];
% the following is a regression equation for the frequency of 1 ghz
eq10=[0.6433   0.1513 3.3664 9.6432 0.0159 0.0959 -0.0929 -0.2028
    -0.0193  -0.361  0  -0.002  -0.0112 0.0087  0.0004];
% the following is a regression equation for the frequency of 1 ghz
eq12=[0.6122   0.1544 3.3268 9.1463 0.0154 0.0912 -0.0876 -0.1955
    -0.0199  -0.3519 -0.0001 -0.002  -0.0108 0.0085  0.0004];
% The following is a list of constants, from eq1 eq2 eq3 eq4 eq5 eq6
constants=[-73.3819 -70.6848   -68.3687   -64.9447   -61.233 -58.301];
% rotates the matrix, this could have been done in the previous form, but
% this allows for easy copy and paste for values from minitab
constants=constants';
% the following arranges the vectors of equations into a matrix.
perm_stand_eq=[eq2; eq4; eq6; eq8; eq10;eq12;];
% the following multiplies the equation matrix by the input values then
% adds the equation constants
perm=perm_stand_eq*inval+constants;
out=perm';
```

Appendix B

Regression Equation Function for Conductivity (MATLAB)

```
function [out]=cond_reg(water,oil,prop,gel)
freq=[1; 2; 3; 4; 5;6]*10^9;
% The vector below  includes all of the possible codependence with respect
% to the 4 input values of water oil propylene glycol and gelatin in grams
inval=[water; oil; prop; gel; water*oil; water*prop; water*gel; oil*prop;
    oil*gel; prop*gel; water*oil*prop; water*oil*gel; water*prop*gel;
    oil*prop*gel; water*oil*prop*gel];
% the following is a regression equation for the frequency of 1 ghz
eq1 =[0.009326  0.005403    0.069668    0.117414    0.000119    0.000549
    -0.000885 -0.002239  -0.000008  -0.002117  -0.000006  -0.000026
    -0.000148 0.000021    0.000006];
% the following is a regression equation for the frequency of 2 ghz
eq2 =[0.02061   0.01062 0.14209 0.27778 0.00026 0.00167 -0.00219
    -0.00492  0.00022 -0.0056 0  -0.00006   -0.00033    0.00001
    0.00001];
% the following is a regression equation for the frequency of 3 ghz
eq3 =[0.03963   0.02071 0.24812 0.53132 0.0005  0.00342 -0.00445
    -0.00936  0.00054 -0.01101    0.00001 -0.00011   -0.00061
    0.00001   0.00002];
% the following is a regression equation for the frequency of 4 ghz


eq4 =[0.06274   0.03352 0.39072 0.83892 0.0008  0.0056  -0.00715
    -0.01496  0.00079 -0.01896    0.00002 -0.00018   -0.00097
    -0.00001 0.00004];
% the following is a regression equation for the frequency of 5 ghz
eq5=[0.08883    0.04688 0.54607 1.17414 0.00113 0.00799 -0.01016
    -0.02119  0.00096 -0.02766    0.00004 -0.00025   -0.00136
    -0.00004 0.00005];
% the following is a regression equation for the frequency of 6 ghz
eq6=[0.8919 0.4746  5.7301  9.9132  0.0119  0.0631  -0.0926
    -0.2092   -0.0063 -0.2525 0  -0.0023 -0.013 0   0.0005];
% The following is a list of constants, from eq1 eq2 eq3 eq4 eq5 eq6
constants=[-0.965082   -2.20514    -4.30058    -6.85627    -9.61554    -81.3173];
% rotates the matrix, this could have been done in the previous form, but
% this allows for easy copy and paste for values from minitab
constants=constants';
% the following arranges the vectors of equations into a matrix.
cond_stand_eq=[eq1; eq2; eq3; eq4; eq5; eq6];
% the following multiplies the equation matrix by the input values then
% adds the equation constants
cond=cond_stand_eq*inval+constants;
out=[cond'];
```

Appendix C

Optimization Script for Dielectric Phantom

```matlab
%% Bruitforce4
%   Bruit force is a section of code that was written to generate matrices
%   of mixtures followed by a matrix containing estimated conductivity and
%   permittivity. the purpose of this program was to use a "guess and check"
%   method to developing a phantom.
%%  set up the range that our equation is valid on
%   true optimization programs didn't handle 4 variables well or the
%   optimization was done in boundless conditions for this experiment it is
%   important to only solve our equation for valid mixtures.
water=40:1:80;
oil=10:1:50;
prop=2:.125:7;
gel=5:.125:10;
tic
index=1;
clear i j k l
n=0;
%% calculating the length of our matrices
%   it take matlab much longer to resize a matrix then it does to overwrite a
%   value this section of code calculates what the length of the final
%   matrix will be.
for i=1:length(water)
    for j=1:length(oil)
        for k=1:length(prop)
            for l=1:length(gel)
                index=index+1;
            end
        end
    end
end
clear i j k l

cond2=zeros(index-1,6);
perm2=zeros(index-1,6);
mix2=zeros(index-1,4);
index=1;
%% creating the matrices
%   by creating these matrices then running the code, the run time of
%   brute force was reduced by 99%
for i=1:length(water)
    for j=1:length(oil)
        for k=1:length(prop)
            for l=1:length(gel)
                cond=cond_reg(water(i),oil(j),prop(k),gel(l));
                perm=perm_reg(water(i),oil(j),prop(k),gel(l));
                perm=perm';
                cond=cond';
                mix=[water(i),oil(j),prop(k),gel(l)];
                n=n+1;
                cond2(index,:)=cond;
                perm2(index,:)=perm;
                mix2(index,:)=mix;
                index=index+1;
            end
        end
    end
end
```

```matlab
end
%% out variables.
%   the remaining variables are cond2, perm2, and mix2 these are used in
%   other programs I have written
 clear water prop perm oil n mix l k j index i gel cond
toc
```

Appendix D

File to data MATLAB script

```matlab
function [out] = filetodata(file_path)
id = fopen(file_path);
% Remove n number of blank lines. At the beginning of program by setting n to the number of blank lines
% or lines of text. This algorithm will not read strings.
n=1;
for m=1:n
    fgetl(id);
end
% a is a variable that we will use to control the number of reads. i is the index of the line we are reading.
a=1;
i=1;
while a
% read is the current line of data that we are processing
    read=fgetl(id);
% This checks to see if there is new data, if there isn't a -1 is returned
    if read==-1
        a=0;
    else
        % Convert the string that is returned to a number than store it in a matrix
        data(i,:)=str2num(read);
        i=i+1;
    end
end
fclose(id);
out=data;
```

Appendix E

Calibration of Sensor Using Regression Analysis (MATLAB)

```matlab
% this was to allow me to minimize the code in the MATLAB m file editor
for n=1:1
% this is the root path were data is stored
file_path='C:\Users\Camerin\Documents\MATLAB\MEMS sensor\Sensor 1 Calibration 3';
% the flowing lines are importing each of the data files, both dielectric properties data and spectrum data
water_dp=filetodata(strcat(file_path,'\water.prn'));
alcohol_dp=filetodata(strcat(file_path,'\alcohol.prn'));
a1_dp=filetodata(strcat(file_path,'\a1.prn'));
a2_dp=filetodata(strcat(file_path,'\a2.prn'));
a3_dp=filetodata(strcat(file_path,'\a3.prn'));
a4_dp=filetodata(strcat(file_path,'\a4.prn'));
a5_dp=filetodata(strcat(file_path,'\a5.prn'));
a6_dp=filetodata(strcat(file_path,'\a6.prn'));
a10_dp=filetodata(strcat(file_path,'\a10.prn'));
a7_dp=filetodata(strcat(file_path,'\a7.prn'));
a8_dp=filetodata(strcat(file_path,'\a8.prn'));
a9_dp=filetodata(strcat(file_path,'\a9.prn'));

water_sa=filetodata(strcat(file_path,'\water.txt'));
alcohol_sa=filetodata(strcat(file_path,'\alcohol.txt'));
a1_sa=filetodata(strcat(file_path,'\a1.txt'));
a2_sa=filetodata(strcat(file_path,'\a2.txt'));
a3_sa=filetodata(strcat(file_path,'\a3.txt'));
a4_sa=filetodata(strcat(file_path,'\a4.txt'));
a6_sa=filetodata(strcat(file_path,'\a6.txt'));
a10_sa=filetodata(strcat(file_path,'\a10.txt'));
a7_sa=filetodata(strcat(file_path,'\a7.txt'));
a8_sa=filetodata(strcat(file_path,'\a8.txt'));
a9_sa=filetodata(strcat(file_path,'\a9.txt'));
end

 % this for loops allows me to minimize the code in the MATLAB m file editor
for n=1:1
% when measuring the data I recorded broad band data, this limits the measurement to the band of interest
water_s1=water_sa(1:101,:);
alcohol_s1=alcohol_sa(1:101,:);
a1_s1=a1_sa(1:101,:);
a2_s1=a2_sa(1:101,:);
a3_s1=a3_sa(1:101,:);
a4_s1=a4_sa(1:101,:);
a6_s1=a6_sa(1:101,:);
a7_s1=a7_sa(1:101,:);
a8_s1=a8_sa(1:101,:);
a9_s1=a9_sa(1:101,:);
a10_s1=a10_sa(1:101,:);
end

 % this for loops allows me to minimize the code in the MATLAB m file editor
for n=1:1
% i represents the index in our data set
```

```matlab
i=1;
% find the maximum intensity in the power spectrum
[value index]=max(a1_s1(:,2));
% recod the max power and frequency for this measurment
measurments(i,:)=a2_s1(index,:);
% increase the index
i=i+1;


% repeat for next measurement
[value index]=max(a2_s1(:,2));
measurments(i,:)=a2_s1(index,:);
i=i+1;

% repeat for next measurement
[value index]=max(a3_s1(:,2));
measurments(i,:)=a3_s1(index,:);
i=i+1;

% repeat for next measurement
[value index]=max(a4_s1(:,2));
measurments(i,:)=a4_s1(index,:);
i=i+1;

% repeat for next measurement
 [value index]=max(a6_s1(:,2));
measurments(i,:)=a6_s1(index,:);
i=i+1;

% repeat for next measurement
 [value index]=max(a7_s1(:,2));
measurments(i,:)=a7_s1(index,:);
i=i+1;

% repeat for next measurement
 [value index]=max(a8_s1(:,2));
measurments(i,:)=a8_s1(index,:);
i=i+1;

% repeat for next measurement
 [value index]=max(a9_s1(:,2));
measurments(i,:)=a9_s1(index,:);
i=i+1;

% repeat for next measurement
 [value index]=max(a10_s1(:,2));
measurments(i,:)=a10_s1(index,:);
i=i+1;

% repeat for next measurement
 [value index]=max(alcohol_s1(:,2));
measurments(i,:)=alcohol_s1(index,:);
end
```

```matlab
% this for loops allows me to minimize the code in the MATLAB m file editor
for n=1:1
% m is an index for the each dielectric property measurement
    m=1;
%because dielectrics are dispersive we would like to find the measurement at the frequency in question
% the we find the index of the measurement with the minimum difference in frequency from the max
% signal found earlier
    [value index]=min(abs(a1_dp(:,1)-measurments(m,1)));
% store these properties
    dielctric(m)=rms(a1_dp(index,[2,3]));
%increment the index
    m=1+m;

%repeat
    [value index]=min(abs(a2_dp(:,1)-measurments(m,1)));
    dielctric(m)=rms(a2_dp(index,[2,3]));
    m=1+m;

%repeat
    [value index]=min(abs(a3_dp(:,1)-measurments(m,1)));
    dielctric(m)=rms(a3_dp(index,[2,3]));
    m=1+m;

%repeat
    [value index]=min(abs(a4_dp(:,1)-measurments(m,1)));
    dielctric(m)=rms(a4_dp(index,[2,3]));
    m=1+m;

%repeat
    [value index]=min(abs(a6_dp(:,1)-measurments(m,1)));
    dielctric(m)=rms(a6_dp(index,[2,3]));
    m=1+m;

%repeat
    [value index]=min(abs(a7_dp(:,1)-measurments(m,1)));
    dielctric(m)=rms(a7_dp(index,[2,3]));
    m=1+m;

%repeat
    [value index]=min(abs(a8_dp(:,1)-measurments(m,1)));
    dielctric(m)=rms(a8_dp(index,[2,3]));
    m=1+m;

%repeat
    [value index]=min(abs(a9_dp(:,1)-measurments(m,1)));
    dielctric(m)=rms(a9_dp(index,[2,3]));
    m=1+m;

%repeat
    [value index]=min(abs(a10_dp(:,1)-measurments(m,1)));
    dielctric(m)=rms(a10_dp(index,[2,3]));
    m=1+m;

%repeat
    [value index]=min(abs(alcohol_dp(:,1)-measurments(m,1)));
    dielctric(m)=rms(alcohol_dp(index,[2,3]));
```

```matlab
%repeat
  [value index]=min(abs(water_dp(:,1)-water(1,1)));
  water_die=rms(water_dp(index,[2,3]));
end
 %normalize the frequency to the oscillation frequency of air
x=(air(1,1)-measurments(:,1));
% preform curve fitting
s1=polyfit(x',dielctric,2)

for i=1:length(Test_f(:,1))
DP_calc(i)=s1(1)*(water_die(1,1)-Test_f(i))^2+s1(2)*(water_die(1,1)-Test_f(i))+s1(3);
end

figure(1)
a=plot(measurments(:,1),dielctric,'*b');
x=sort(measurments(:,1));
calc=s1(1)*(air(1,1)-x).^2+s1(2).*(air(1,1)-x)+s1(3);
hold on
b=plot(x,calc,'r');
legend([a b],'Calibration Data Points','Curve of best fit')
title('Sensor 1 Calibration')
ylabel('{\epsilon}_{r}')% label
xlabel('Frequency')     % label
```

REFERENCES

[1]   S. W. Fletcher and J. G. Elmore, "Mammographic screening for breast cancer," *The New England Journal of Medicine*, vol. 384, pp. 1672-1680, Apr. 2003.

[2]   E. C. Fear, S. C. Hagness, P. M. Meaney, M. Okoniewski, and M. A. Stuchly, "Enhansing breast tumor detection with near-field imaging," *Microwave Magazine, IEEE*, vol. 3, no. 1, pp. 48-56, Mar. 2002.

[3]   E. C. Fear, P. M. Meaney, and M. A. Stuchly, "Microwaves for breast cancer detection?," *IEEE Potentials*, vol. 22, no. 1, pp. 12-18, Feb./Mar. 2003.

[4]   N. Howlader, Noone A. M., M. Krapcho, N. Neyman, R. Aminou, W. Waldron, S. F. Altekruse, C. L. Kosary, J. Ruhl, Z. Tatalovich, H. Cho, A. Mariotto, M. P. Eisner, D. R. Lewis, H. S. Chen, E. J. Feuer, K. A. Cronin, and B. K. Edwards, "SEER cancer stastics review 1975-2008," National Cancer Institute, Bethesda, MD, 2011.

[5]   C. Gabriel, S. Gabriel, and E. Corthout, "The Dielectric properties of biological tissues: I. Literature survey," *Physics in Medicine and Biology*, pp. 2231-2249, 1996.

[6]   S. Gabriel, R. W. Lau, and C. Gabriel, "The dielectric properties of biological tissues: II. Measurements in the frequency range 10 Hz to 20 GHz," *Physics in Medicine and Biology*, vol. 41, no. 11, pp. 2251-2269, Nov. 1996.

[7]   S. Gabriel, R. W. Lau, and C. Gabriel, "The dielectric properties of biological tissues: III Parametric models for the dielectric spectrum of tissues," *Physics in Medicine and Biology*, vol. 41, no. 11, pp. 2271-2293, 1996.

[8]   M. Lazebnick, E. L. Madsen, G. R. Frank, and S. C. Hagness, "Tissue-mimicing phantom materials for narrowband and ultrawideband microwave applications," *Physics in Medicine and Biology*, vol. 50, pp. 4245-4258, 2005.

[9]   A. Mashal, F. Gao, and S. C. Hagness, "Heterogeneous anthropomorphic phantoms with realistic dielectric properties for microwave breast imaging experiments," *Microwave and Optical Technology Letters*, vol. 53, no. 8, pp. 1896-1902, Aug. 2011.

[10] M. Ostarahimi, R. Reopelle, A. Vahedi, F. Safari, and S. Noghanian, "A heterogeneous breast phantom for microwave breast imaging," in *Annual International Conference of the IEEE Engineering in Medicine and Biology Society*, Minneapolis, USA, 2009, pp. 2727-2730.

[11] J. C. Y. Lai, C. B. Soh, E. Gunawan, and K. S. Low, "Homogeneous and heterogeneous breast phantoms for ultra-wideband imaging applications," *Progress In Electromagnetics Research*, vol. 100, pp. 397-415, 2010.

[12] C. Polk and E. Postow, *Handbook of Biological Effects of Electromagnetic Fields*, 2nd ed., C. Polk and E. Postow, Eds. US: CRC press, 1996.

[13] T. A. Whitman, J. C. Forrest, M. T. Morgan, and M. R. Okos, "Electrical measurement for detecting early postmortem changes in porcine muscle," *Journal of Animal Sciences*, vol. 74, no. 1, pp. 80-90, Jan. 1996.

[14] H. J. Swatland, "Postmortemchanges in electrical capacitance and resistivity of pork," *Journal of Animal Science*, vol. 51, no. 5, pp. 1108-1112, Nov. 1980.

[15] W. Hayt and J. Buck, *Engineering Electromagnetics*, seventh edition ed. New York, US: Mc Graw Hill, 2006.

[16] A. M. Campbell and D. V. Land, "Dielectric properties of female human breast tissue measured *in vitro* at 3.2 GHz," *Physics in Medicine and Biology*, pp. 193-210, 1992.

[17] U. Kaatze, "Techniques for measuring the microwave dielectric properties of materials," *Metrologia*, pp. S93-S113, 2010.

[18] B. B. Owen, R. C. Miller, C. E. Milner, and H. L Cogan, "The dielectric constant of water as a function of temperature and pressure," *The Journal of Physical Chemistry*, vol. 65, no. 11, pp. 2065-2070, Nov. 1961.

[19] K. B. Yu, S. G. Ogourtsov, V. G. Belenky, A. B. Maslenikov, and A. S. Omar, "Accurate microwave resonant method for complex permittivity measurements of liquids [biological]," *IEEE Transactions on Microwave Theory Techniques*, vol. 48, no. 11, pp. 2159-2164, Nov. 2000.

[20] J. Cho, J. Yoon, S. Cho, K. Kwon, S. Lim, D. Kim, E. S. Lee, C. Hwan K., J. Wook C., C. Cheon, and Y. Kwon, "*In-vivo* measurements of the dielectric properties of breast carcinoma xenografted on nude mice," *Internation Journal of Cancer*, pp. 593-598, 2006.

[21]   A. P. O'Rourke, M. Lazebnik, J. M. Betram, M. C. Converse, S. C. Hagness, J. G. Webster, and D. M. Mahvi, "Dielectric properties of human normal, malignant and cirrhotic liver tissues: *in vivo* and *ex vivo* measurements from .5 to 20 GHz using a precision open-ended coaxial probe," *Pysics in Medicine and Biology*, pp. 4707-4719, 2007.

[22]   A. Peyman, S. J. Holden, S. Watts, R. Perrott, and C. Gabriel, "Dielectric properties porcine cerebrosspinal tissues at microwave frequencies: *in vivo*, *in vitro* and systematic variation with age," *Physics in Medicine and Biology*, pp. 2229-2245, 2007.

[23]   M. Lazebnik, L. McCartney, D. Popovic, C. B. Watkins, M. J. Lindstrom, J. Harter, S. Sewall, A. Magliocco, J. H. Booske, and S. C. Hagness, "A large-scale study of the ultrawideband microwave dielectric properties of normal breast tissue obtained from reduction surgeries.," *Physics in Medicine and Biology*, vol. 52, pp. 2637-2656, 2007.

[24]   D. Popovic, L. McCartney, C. Beasley, M. Lazebnik, M. Okoniewski, S. C. Hagness, and J. H. Booske, "Precision open-ended coaxial probes for *in vivo* and *ex vivo* dielectric spectroscopy of biological tissues at microwave frequencies," *IEEE Transactions on Microwave Theory and Techniques*, pp. 1713 - 1722, May 2005.

[25]   G. Heath, "Basic immunology," Association of Optometrists., London, 2002.

[26]   L. Pruit. (2007, Aug.) Uc Berkeley Chanel. [Online]. http://www.youtube.com/watch?v=p4QRSUrhQzA

[27]   J. P. Desborough, "The stress response to trauma and surgery," *British Journal of Anaestesia*, vol. 85, no. 1, pp. 109-117, Mar. 2000.

[28]   X. Fu, W. Chen, S. Ye, Y. Tu, Y. Tang, D. Li, H. Chen, and K. Jiang, "A wireless implantable sensor network system for *in vivo* monitoring of physiological signals," *IEEE Transactions on Information Technology in Biomedicine*, vol. 15, no. 4, pp. 577-584, Jul. 2011.

[29]   F. Chen, A. P Chandrakasan, and V. Stojanović, "A signal-agnostic compressed sensing acquisition system for wireless and implantable sensors," in *Custom Integrated Circuits Conference (CICC)*, San Jose, CA, sept 2010, pp. 1-4.

[30]   E. Y. Chow, C. L. Yang, A. Chelbowski, S. Moon, W. J. Chappell, and P. P. Irazoqui, "Implantable wirelss telemetry boards for in vivo transocular transmission," *IEEE Transactions on Microwave Theory and Techniques*, vol. 56, no. 12, pp. 3200-3208, Dec. 2008.

[31] E. Y. Chow, C. L. Yang, A. Chelbowski, W. J. Chappell, and P. P. Irazoqui, "Miniature antenna for RF telemetry through ocular tissue," in *Microwave Symposium Digest*, Atlanta, GA, 2008, pp. 1309-1312.

[32] E. Y. Chow, A. L. Chelbowski, S. Chakraborty, W. J. Chappell, and P. P. Irazoqui, "Fully wirelss implantable cardiovascular pressure monitor integrated with medical stent," *IEEE Transactions on Biomedical Engineering*, vol. 57, no. 6, pp. 1487-1496, Jun. 2010.

[33] M. Yvanoff and J. Venkataraman, "A feasibility study of tissue characterization using LC sensors," *IEEE Transactions on Antennas and Propagaions*, vol. 57, no. 4, pp. 885-893, Apr. 2009.

[34] P. G. Sarrigiannis, R. P. Kennett, S. Read, and M. E. Farrugia, "Single-fiber EMG with a concentric needle electrode: validation in myasthenia gravis," *Muscle & Nerve*, vol. 33, no. 1, pp. 61-65, Sep. 2005.

[35] Y. K. Song, D. A. Borton, S. Park, W. R. Patterson, C. W. Bull, F. Laiwalla, J. Mislow, J. D. Simeral, and J. P. Donoghue, "Active microelectronic neurosensor arrays for implantable brain communication interfaces," *IEEE Transactions on Neural System Rehabilitation*, vol. 17, no. 4, pp. 339-345, Aug. 2010.

[36] P. J. Chen, D. C. Rodger, S. Saati, M. S. Humayun, and Y. C. Tai, "Microfabricated implantable parylene-based wireless passive intraocular preassure sensor," *Journal of Microelectromechanical Systems*, vol. 17, no. 06, pp. 1342-1349, Dec. 2008.

[37] M. D. Pearlman and D. Viano, "Automobile crash simulation with the first pregnant crash test dummy," *American Journal of Obstetrics and Gynecology*, vol. 175, no. 4, pp. 977-981, Oct. 1996.

[38] E. L. Madsen, J. A. Zagzebski, R. A. Banjavie, and R. E. Jutila, "Tissue mimicking materials for ultrasound phantoms," *Medical Physics*, vol. 5, no. 5, pp. 391-394, May 1978.

[39] G. Salvador and S. M. Vecchi, "Experimental tests of microwave breast cancer detection on phantom," *IEEE Transactions on Antenna and Propagations*, vol. 57, no. 6, pp. 1705-1712, 2009.

[40] J. M. Sill and E. C. Fear, "Tissue sensing adaptive radar for breastcancer detection—Experimental investigation of simple tumor models," *IEEE Transactions Microwave Theory Techniques*, vol. 53, no. 11, pp. 3312–3319, Nov. 2005.

[41]   P. M. Meaney, N. K. Yagnamurthy, and K. D. Paulsen, "Pre-scaled two-parameter Gauss-Newton image reconstruction to reduce property recovery imbalance," *Physics in Medicine and Biology*, vol. 47, no. 7, pp. 1101–1119, Apr. 2002.

[42]   M. Klemm, J. A. Leendertz, D. Gibbins, I. J. Craddock, Preece A., and R. Benjamin, "Microwave radar-based breast cancer detection: Imaging in inhomogeneous breast phantoms," *IEEE Antennas Wireless Propag Letters*, vol. 8, pp. 1349-1352, 2009.

[43]   D. E. Dupuy, R. Hong, B. Oliver, and S. N. Goldberg, "Radiofrequency ablation of spinal tumors: temperature," *American Journal of Roentgenology*, vol. 175, no. 5, pp. 1263-1266, Nov. 2000.

[44]   J. M. Lee, J. K. Han, S. H. Kim, K. L. Sohn, K. H. Lee, S. K. Ah, and B. I. Choi, "A cmparative experimental study of the *in-vitro* efficiency of hypertonic saline-enhanced hepatic bipolar and monopolar radiofrequency ablation," *Korean Journal of Radiology*, vol. 4, no. 3, pp. 136-139, Sep. 2003.

[45]   T. Dickfeld, H. Calkins, M. Zviman, K. Risuhi, G. Meininger, L. Lickfett, R. Berger, H. Halperin, and S. B. Solomon, "Anatomic stereotactic catheter ablation on three-dimensional magnetic resonance images in real time," *Journal of the American Heart Association*, vol. 108, pp. 2407-2413, Oct. 2003.

[46]   S. Bharat and T. Varghese, "Radio-frequency ablation electrode displacement elastography: A phantom study," *Medical Physics*, vol. 35, no. 6, pp. 2432-2442, Jun. 2008.

[47]   M. D. Sherar, A. S. Gladman, S. R. H. Davidson, J. Trachtenberg, and M. R. Gertner, "Helical antenna arrays for interstitial microwave thermal therapy for prostate cancer: tissue phantom testing and simulations for treatment," *Physics in Medicine and Biology*, vol. 46, no. 7, pp. 1905-1918, Jul. 2001.

[48]   L. Chung-Huan, E. Ofli, N. Chavannes, and N. Kuster, "Effects of hand phantom on mobile phone antenna performance," *IEEE Transactions on Antennas and Propagation*, vol. 57, no. 9, pp. 2763-2770, Sep. 2009.

[49]   B. B. Beard, W. Kainz, T. Onishi, T. Iyama, S. Watanabe, O. Fujiwara, J. Wang, G. Bit-Babik, A. Faraone, J. Wiart, A. Christ, N. Kuster, A. K. Lee, H. Kroeze, M. Siegbahn, J. Keshvari, H. Abrishamka, W. Simon, D. Manteuffel, and N. Nikoloski, "Comparisons of computed mobile phone induced SAR in the SAM phantom to that in anatomically correct models of the human head," *IEEE Transactions on Electromagnetic Compatibility*, vol. 48, no. 2, pp. 397-407, May 2006.

[50] W. Kainz, J. P. Casamento, P. S. Ruggera, D. D. Chan, and D. M. Witters, "Implantable cardiac pasemaker compatibility test in a novel security system simulator," *IEEE Transaction on Biomedical Engineering*, vol. 52, no. 3, pp. 520-530, Mar. 2005.

[51] B. A. Schueler, T. B. Parrish, J. C. Lin, B. E. Hammer, B. J. Pangrle, E. R. Ritenour, J. Kucharczyk, and C. L. Truwit, "MRI compatiblity and visibility assessment of implantable medical devices," *Journal of Magnetic Resonance Imaging*, vol. 9, no. 4, pp. 596-603, Apr. 1999.

[52] I. Unal, B. Turetken, K. Surmeli, and C. Canbay, "An experimental microwave imaging system for breast tumor detection on layerd phantom model," in *URSI General Assembly*, Istanbul Turkey, 2011, pp. 1-4.

[53] M. J. Schroeder, S. Anupama, and R. M. Nelson, "An analysis on the role of water content and state on effective permittivity using mixing formulas," *Journal of Biomechanics, Biomdical, and Biophysical Engineering*, vol. 2, no. 1, Jun. 2008.

[54] J. Z. Bao, M. L. Swicord, and C. C. Davis, "Microwave dielectric characterization of binary mixtures of water, methanol, and ethanol," *Journal of Chemical Physics*, vol. 104, no. 12, Mar. 1996.

[55] N. William, *Principles of Statistics for Engineers and Scientists*. New York, NY: McGraw-Hill, 2010.

[56] D. C. Montgomery, G. C. Runger, and N. F. Hubele, *Engineering Statistics*. Hoboken: John Wiley & Sons, 2007.

[57] Minitab inc. (2010, Dec.) Minitab. [Online]. http://www.minitab.com/en-US/default.aspx

[58] Mathworks. (2010, Dec.) Mathworks. [Online]. http://www.mathworks.com/products/matlab/

[59] R. J. Halter, T. Zhou, P. M. Meaney, A. Hartov, R. R. Barth Jr., K. M. Rosenkranz, W. A. Wells, C. A. Kogel, E. J. Rizzo, and K. D. Paulsen, "The correlation of *in vivo* and *ex vivo* tissue dielectric properties to validate electromagnetic breast imaging: initial clinical experience," *Physiological Measurement*, vol. 30, no. 6, pp. S121-S136, Jun. 2009.

[60] H. Hammer, "Analytical model for comb-capacitance fringe fields," *Journal of Microelectromechanical Systems*, vol. 19, no. 1, pp. 175-182, Feb. 2010.

[61] Ansys, Ansoft Designer, 2012, http://www.ansys.com/Products/Simulation+Technology/Electromagnetics/Ansoft+Designer.